PB 208 233

MICROWAVE ENERGY ABSORPTION in TISSUE

ENVIRONMENTAL PROTECTION AGENCY
Office of Research and Monitoring

62

Reproduced by
NATIONAL TECHNICAL
INFORMATION SERVICE
Springfield, Va. 22151

ENVIRONMENTAL PROTECTION AGENCY
OFFICE OF RESEARCH AND MONITORING
TWINBROOK RESEARCH LABORATORY

The technical publications issued by the Twinbrook Research Laboratory report results of intramural and contractor projects. A limited number of the reports are distributed to regional, state, and local radiological health agencies, to universities and libraries, to other government and private agencies, and to interested individuals.

The Twinbrook Research Laboratory technical reports listed below are available from the National Technical Information Service, Springfield, Virginia 22151. Microfiche copies are $0.95 and paper copies are $3.00 unless otherwise noted. Please refer to the PB number when ordering the reports.

PB 207 079	Krypton 85: A Review of the Literature and an Analysis of Radiation Hazards (January 1972)
PB	Microwave Energy Absorption in Tissue (February 1972)

MICROWAVE ENERGY ABSORPTION in TISSUE

Richard A. Tell

Twinbrook Research Laboratory
12709 Twinbrook Parkway
Rockville, Maryland 20852

FEBRUARY 1972

ENVIRONMENTAL PROTECTION AGENCY
Office of Research and Monitoring
Washington, D.C. 20460

DISCLAIMER

The mention of commercial preparations or products in no way constitutes endorsement by the U.S. Environmental Protection Agency or its affiliates.

FOREWORD

The Twinbrook Research Laboratory plans and conducts research studies related to the impact of environmental radiation on the health and well-being of mankind. Through investigations of the biological effects of both ionizing and nonionizing radiation, the Laboratory seeks to define potentially hazardous levels of radiation on which to base criteria for the development of environmental exposure standards.

These studies rely heavily on an ability to physically specify the extent of irradiation in experimental subjects. This report concerns technical aspects of the dosimetry problem associated with biological subjects exposed to energy in the microwave region of the electromagnetic spectrum.

The author discusses the dielectric properties of various tissues and explains the approaches used to calculate wave impedance throughout multilayered tissue systems. The coupling factor between exposure and absorbed energy is derived; energy distribution, its development as heat, and its relation to temperature rise in tissues is discussed.

Additional information of this type is sought on a continuing basis and the interest and comments of individuals concerned with various aspects of radiation protection of man and his environment are solicited.

William A. Mills

William A. Mills, Ph.D.
Director
Twinbrook Research Laboratory

CONTENTS

Foreword iii
Abstract vii
Acknowledgments viii
Introduction 1
Dielectric Properties of Tissues 4
Impedance Calculations in Multilayered Tissue Systems 9
Total Dose Absorbed by System 15
Dose Distribution within System 23
Comments on Temperature Rise in Tissues 39
Summary and Conclusions 45
References 47

Appendixes

A. Verification of Identity: $\tan \delta = \frac{60}{K_m'}$ 51

B. Derivation of Wavelength Reduction in a Dielectric Material . 52

C. Verification that $\alpha\beta = \frac{\mu\sigma\omega}{2}$ 53

Tables

1. Relative Dielectric Constant and Resistivity of Body Tissues at 37° C 6
2. Temperature Coefficient of Relative Dielectric Constant and Specific Resistance of Body Tissues in Percent per Degree. . 9
3. Dielectric Properties of Water at Selected Frequencies and Temperatures 10
4. Parameters for Tissues in Figure 7 17
5. Densities and Heat Capacities of Various Tissues 41

Figures

1. Field Strength and Power Density in Free Space 2
2. Plane Slab Model Tissue System 3
3. Complex Dielectric Constant of Skin, Fat, and Muscle 7
4. Vector Representation of Z_m^* 13
5. Vector Representation of K_m^* 13
6. Propagation Constant of Skin, Fat, and Muscle 14
7. Model Configuration for Smith Chart Solution 18
8. Smith Chart Solution 19

9. 915 MHz Power Absorption in Tissues 21
10. 2450 MHz Power Absorption in Tissues 21
11. 8500 MHz Power Absorption in Tissues 22
12. Relative Heat Development Rate in Two-Layer Model 28
13. Relative Heat Development Rate in Three-Layer Model 30
14. Thermal Dose Distribution at 915 MHz 33
15. Thermal Dose Distribution at 2450 MHz 34
16. Thermal Dose Distribution at 8500 MHz 37
17. Effect of Skin Thickness on Fraction of Total Heat Developed in Skin and Fat 38
18. Maximum Tissue Temperature Elevation in Two-Component System 43
19. Maximum Tissue Temperature Elevation in Three-Component System 43

BIBLIOGRAPHIC DATA SHEET	1. Report No.	2.	3. Recipient's Accession No.
4. Title and Subtitle Microwave Energy Absorption in Tissue			5. Report Date February 1972 6.
7. Author(s) Richard A. Tell			8. Performing Organization Rept. No.
9. Performing Organization Name and Address Twinbrook Research Laboratory 12720 Twinbrook Parkway Rockville, Maryland 20852			10. Project/Task/Work Unit No. 11. Contract/Grant No.
12. Sponsoring Organization Name and Address Environmental Protection Agency Office of Research and Monitoring			13. Type of Report & Period Covered 14.

15. Supplementary Notes

16. Abstracts

Various approaches may be used in describing microwave interactions with animal systems. This paper is intended as a guide to several dosimetric techniques useful with a slab model configuration of biological tissues. A detailed account is given of the calculational concepts, gathered from the literature, which are used to determine the degree of power absorption within such tissue systems as well as the spatial distribution of this absorbed dose as heat and consequently, the tissue temperature elevations which may be experienced in the model. Both a graphic-analytic technique using the Smith chart and a mathematical derivation of the appropriate computing formulas are given. Adequate derivation of the appropriate computing formulas are given. Adequate reference is made to direct the reader to pertinent literature concerning other models and mathematical methods involved in microwave dosimetry.

17. Key Words and Document Analysis. 17a. Descriptors

Microwave Energy
Energy Absorption
Biological Tissue
Energy distribution
Multilayer Model

17b. Identifiers/Open-Ended Terms

17c. COSATI Field/Group

18. Availability Statement	19. Security Class (This Report) UNCLASSIFIED	21. No. of Pages
	20. Security Class (This Page UNCLASSIFIED	22. Price

USCOMM-DC 40329-P71

ABSTRACT

Various approaches may be used in describing microwave interactions with animal systems. This paper is intended as a guide to several dosimetric techniques useful with a slab model configuration of biological tissues. A detailed account is given of the calculational concepts, gathered from the literature, which are used to determine the degree of power absorption within such tissue systems as well as the spatial distribution of this absorbed dose as heat and consequently, the tissue temperature elevations which may be experienced in the model. Both a graphic-analytic technique using the Smith chart and a mathematical derivation of the appropriate computing formulas are given. Adequate reference is made to direct the reader to pertinent literature concerning other models and mathematical methods involved in microwave dosimetry.

INTRODUCTION

Interaction of electromagnetic (EM) energy with a material may be characterized by the various mechanisms that are active during the interaction process. Some of these mechanisms convert radio frequency (RF) and microwave energy to heat within the target material; others are so-called field evoked force effects that are not necessarily associated with a temperature rise in the interacting medium. Although field evoked force effects, which include pearl chain formation, particle orientation, molecular resonance, and membrane excitation, have been studied in some detail (1-4), experiments aimed at finding biophysical responses to these phenomena without the presence of significant thermal effects have proved difficult. Consequently, most biological effects research in the United States has been based on the assumption that the primary effective mechanism involved is heating induced by EM energy throughout the tissue. This approach is based on the practicality of the situation; subtle nonthermal effects have been observed both here and abroad (5-7), principally in the U.S.S.R. where a rather complete compilation of this type of information has recently been made (8). However, the theories developed to explain these effects (primarily information theory) have not been substantially subjected to experiment to ensure widespread acceptance of their application in this case. Accordingly, RF and microwave dosage measurements (absorbed energy) have been tied to the Joule heating effect and attempts to measure and predict the degree of local heat developed throughout the irradiated object. This is not to say that other parameters, such as electric field strength within the tissue or surface current density might not provide a better measurement of absorbed dose, but other reasons such as lack of instrumentation and the subjective nature of biological interpretation lead one, at least presently, generally back to the heat concept. To this end this report discusses the relationship between exposure and absorbed energy and the conversion of this energy to heat in various tissue systems.

Because of the nature of thermal regulation in animals, dose rate is the most useful term for relating biophysical responses to RF and microwave energy exposure. That is, at low energy input rates, below the intrinsic heat dissipation capability of the animal, negligible responses may occur. At greater energy deposition rates, biological responses may be indicative of stress on the animal's thermal regulatory system. Fortunately, at microwave frequencies a common expression for radiation intensity, because of technical reasons, is in terms of free space exposure dose rate or power density, i.e. mW/cm^2. Other measurements such as electric field strength (volts/meter), usually (see Figure 1) used at radio frequencies, are

convertible to power density. Thus. if an expression describing the absorption efficiency and power absorption pattern for a particular biological system can be obtained, then the resultant heating rate at a specific point may be directly established.

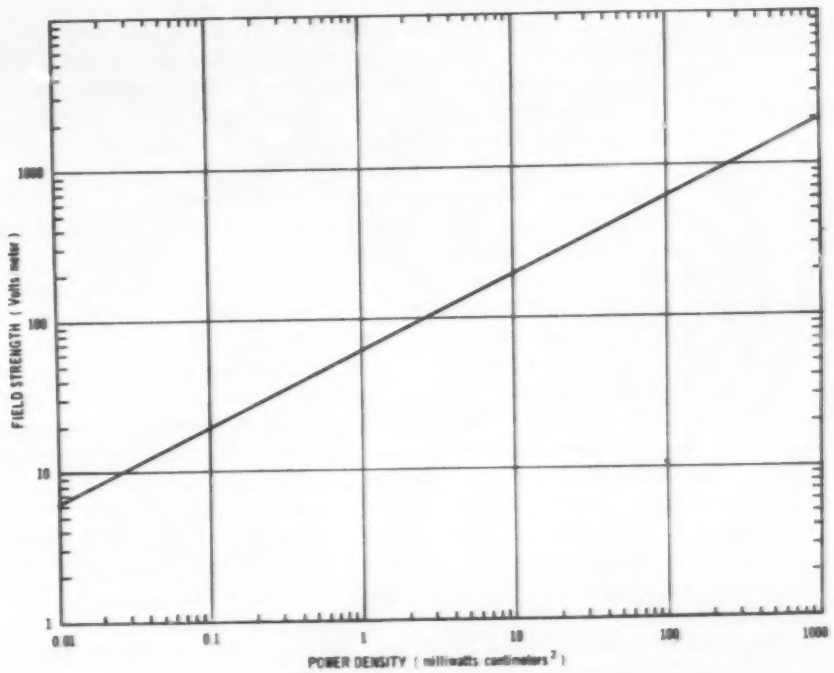

Figure 1. Field Strength and Power Density in Free Space.

The problem of microwave dosimetry in humans and laboratory animals is severely complicated by the critical and highly variable relationship of energy absorption upon tissue parameters. Unlike high-energy photons such as x rays, microwaves may be strongly reflected by an interface between two different tissues. The total energy or power extracted from an incident beam of microwaves may vary from a small amount to essentially 100 percent depending greatly on the particular dielectric properties and the physical configuration of the tissues. Consequently, unlike ionizing radiation dosimetry, no fixed conversion factors can be developed

which relate, in general, exposure measurements in the free field to absorbed dose. On the contrary, every animal or specific absorber, because of its own particular makeup, has its own conversion factor.

At first sight, because of this highly variable coupling of animal with electromagnetic field, the problem of dosimetry appears unmanageable, and one is inclined to adhere solely to specifying free field exposures. However, if the interactions between EM energy and simplified tissue systems are examined carefully, one can gain an insight into the heat development process and spatial distribution of this heat. From here one may examine more complex models of systems in an attempt to describe the actual energy deposited in the system.

For the sake of simplicity in analysis and explanation the system described in this paper consists of a series of planar slabs that are arranged to simulate the configuration of typical human tissues. These layers are depicted by Figure 2 and are assumed to be infinite

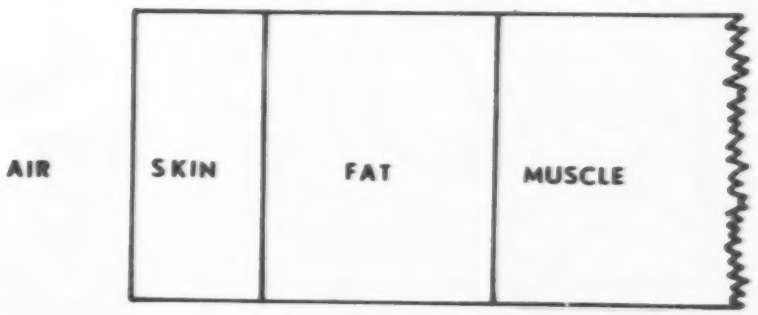

Figure 2. A Section of Plane Slab Model Tissue System.

in extent. Also, the base layer of muscle tissue is assumed to be semi-infinite in depth, i.e., there are no underlying reflective surfaces to which a wave might penetrate. This constraint is fulfilled in most practical cases by the relatively high absorption characteristics of the muscle tissue. A further supposition is that the test system is exposed to plane electromagnetic waves.

This report details the calculations used in describing EM energy absorption and distribution within plane slab model tissue systems. The application of these procedures has been reported

previously in numerous other publications (9-12). In this report the calculations are extended to different frequencies and combinations of tissue configurations with sufficient explanation to enable one to carry out computations for specific conditions. First, the dielectric properties of various tissues are discussed, including factors that influence their values and techniques used in their measurement. Secondly, the approach used to calculate the wave impedance throughout multilayered tissue systems is explained. Once this is accomplished, the coupling factor between exposure and absorbed energy is derived. After the total dose is found, the determination of its distribution as heat is discussed with emphasis on ultimately relating heat development to temperature rise within the tissues. The report is concluded with comments on application of the techniques to experimental studies, a description of other types of models and theoretical approaches, and a summary of the results obtained in this paper.

DIELECRTRIC PROPERTIES OF TISSUES

Dielectric response of a material placed in a sinusoidal field may be described by two parameters, the complex permittivity, (ε^*), and complex permeability, (μ^*). These two parameters relate to the dielectric's ability to store electric and magnetic energy. Customarily, the complex permittivity is expressed in the form,

$$\varepsilon^* = \varepsilon' - j\varepsilon''$$

where ε', or the dielectric constant, represents the dielectric's storage capacity for electric field energy and ε'', the loss factor, represents the loss of electric field energy due to frictional losses by charge flow and dipolar rotation. In the MKSC system of units, the dielectric constant for vacuum is designated ε_o and has a value of 8.854×10^{-12} farads/meter. Generally one works in terms of relative measures of a materials permittivity, i.e., the ratio of the actual permittivity of the material to that of vacuum,

$$\frac{\varepsilon^*}{\varepsilon_o} = K^*$$

where $K^* = K' - jK''$. K' is the relative dielectric constant and K'' is the relative loss factor, both quantities being dimensionless. A similar relation exists for the complex relative permeability,

$$K^*_{mag} = \frac{\mu^*}{\mu_o} = K'_{mag} - jK''_{mag}$$

where $\mu_o = 1.257 \times 10^{-6}$ henry/meter. However, because biological tissues represent essentially no magnetic perturbation to EM fields, μ^* is generally set equal to μ_o; hence, the complex relative permittivity is the parameter of interest in most dosimetric calculations.

The relative permittivities of biological materials usually are characterized as being frequency dependent. This dependency is characterized, for most biological tissue, by the evidence of three regions of dispersion. In the first of these regions, below 300-400 MHz, the cell membranes, which act as layers of high capacity and resistance, become short circuited as the frequency is increased and permit the cell's contents to participate in current conduction. Thus, the capacitance and specific resistance of the tissue decrease as frequency increases in this region. Dispersion beyond 3000-6000 MHz is due to rotation of water molecules that are contained in most tissues. Electrical polarity of the water molecule causes it to rotate in unison with the applied electrical field until the inertia of the molecule becomes prohibitively large. At this critical frequency, approximately 20,000 MHz for water, both the resistance and dielectric constant decrease. The remaining intermediate dispersion region represents a frequency range (~400 to 4,000 MHz) in which cell membranes no longer affect tissue properties, yet the water molecule is not strongly frequency dependent. Detailed accounts of the theory of dielectrics can be found in the literature (13-15).

A collection of dielectric data by Schwan (16) is reproduced in Table 1 where values of relative dielectric constant and the resistivity of various tissues are entered. Several other sources of dielectric data for biological tissues are available (17, 18). Resistivity, ρ, or its reciprocal, the dielectric conductivity, $\sigma = 1/\rho$, is sometimes given in lieu of the relative loss factor K''. The units of ρ in Table 1 are ohm-meters allowing ready conversion of ρ to the relative loss factor through the relation

$$K'' = \frac{1}{\rho\omega\varepsilon_o} = \frac{\sigma}{\omega\varepsilon_o}$$

where: K'' = relative loss factor (dimensionless)

ρ = resistivity (sometimes called specific resistance) in units of ohm-meters

ω = angular frequency = 2π f (f in units of Hz)

ε_o = permittivity of vacuum = 8.854×10^{-12} F/m.

σ = conductivity (mhos/meter) $(\text{ohm-meters})^{-1}$

TABLE 1. RELATIVE DIELECTRIC CONSTANT AND RESISTIVITY OF BODY TISSUES AT 37° C[a]

Tissue	Frequency, MHz								
	25	50	100	200	400	700	1000	3000	8500
				Relative Dielectric Constant, K'					
Muscle	103-115	85-97	71-76	56	52-64	52-53	49-52	45-48	40-42
Heart Muscle				59-63	52-56	50-55			
Liver	136-138	88-93	76-79	50-56	44-51	42-51	46-47	42-43	34-38
Spleen	200	135-140	100-101						
Kidney	200	119-132	87-92	62	53-55	50-53			
Lung				35	35	34			
Skin			65		46-48		43-46	40-45	36
Brain	160	110-114	81-83						
Fat		11-13					5.3-7.5	3.9-7.2	3.5-4.5
Bone Marrow		6.8-7.7		4.5-7.5	4-7		4.3-7.3	4.2-5.8	4.4-5.4
				Resistivity ρ, ohm-meters					
Muscle		1.13-1.47		0.95-1.05	0.85-0.90	0.73-0.79	0.75-0.79	0.43-0.46	0.12
Heart Muscle				0.95-1.15	0.85-1.00	0.78-0.95			
Liver	1.85-2.10	1.73-1.95	1.54-1.79	1.10-1.50	1.05-1.30	0.85-1.15	0.98-1.06	0.49-0.50	0.15-0.17
Spleen		1.28-1.51							
Kidney		0.90-1.45		0.90	0.85	0.76-0.77			
Lung		2.60-4.50		1.60	1.40	1.30			
Skin			1.20-1.40		1.10-1.30		0.90-1.10	0.37-0.50	0.14
Brain	2.20	1.90-2.10	1.80-1.95						
Fat		17.00-25.00		10.50-35.00	9.00-28.00		6.70-12.00	4.40-9.00	2.40-3.70
Bone Marrow		28.00-50.00					10.00-23.00	4.45-8.60	2.10-6.00

[a]Data taken from reference 16

Mean values of K' and K'' (derived from Table 1) for skin, fat, and muscle tissues are plotted in Figure 3, over a frequency range of 400 to 8500 MHz. The range of ρ, and consequently K'', for fat is indicative of the highly variable water content in fatty tissue.

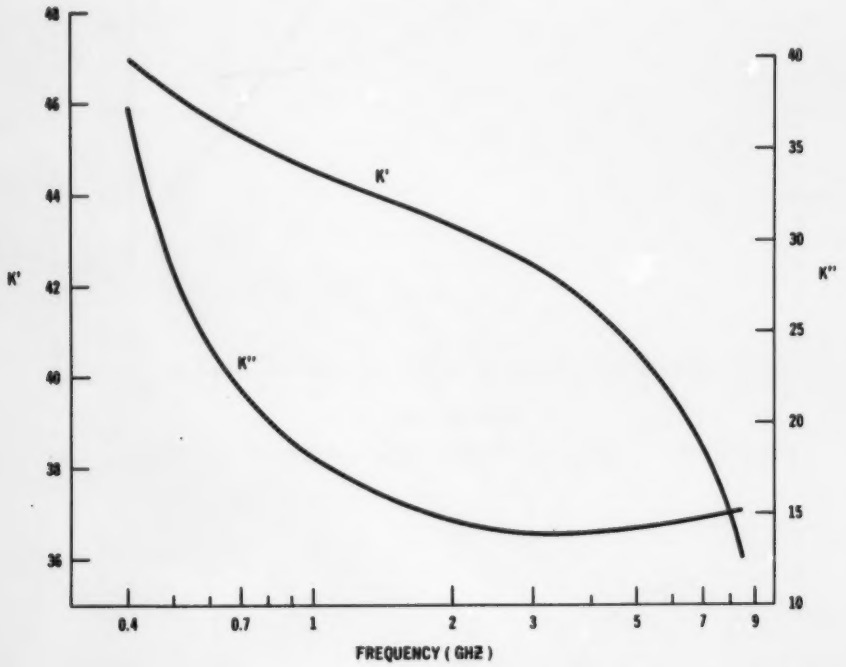

Figure 3A. Complex Dielectric Constant of Skin.

Dielectric parameters vary also with temperature of the material. Table 2 gives temperature coefficients of dielectric constants and resistivities for various tissues at several different frequencies. In general the dielectric constant is affected statistically less by temperature change than is the resistivity (19). The temperature dependence of K' and K'' for water is shown in Table 3.

Generally, the dielectric constant is essentially independent of tissue temperature and the loss factor K'' shows small (about 2 percent/^{o}C) changes with temperature over the region of interest

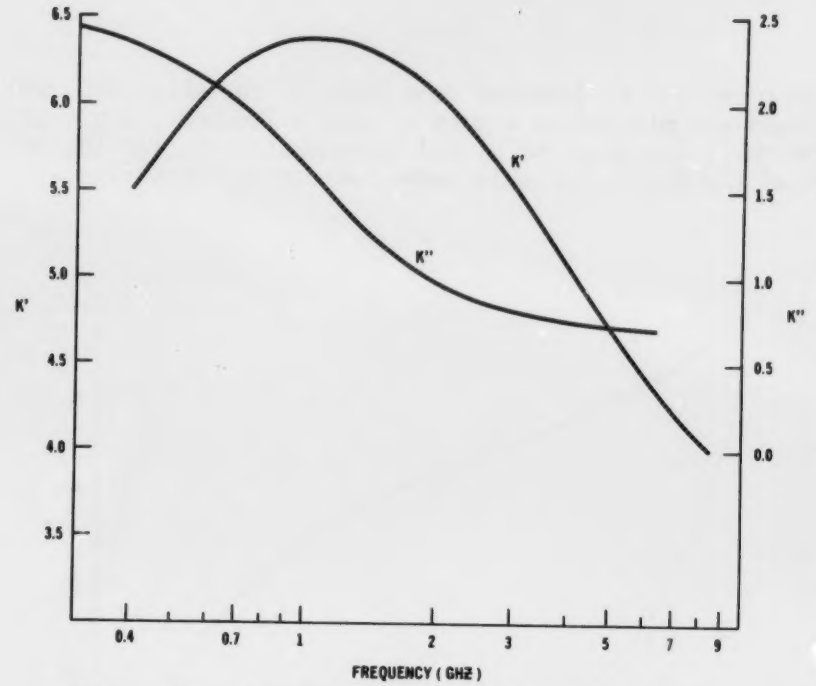

Figure 3B. Complex Dielectric Constant of Fat.

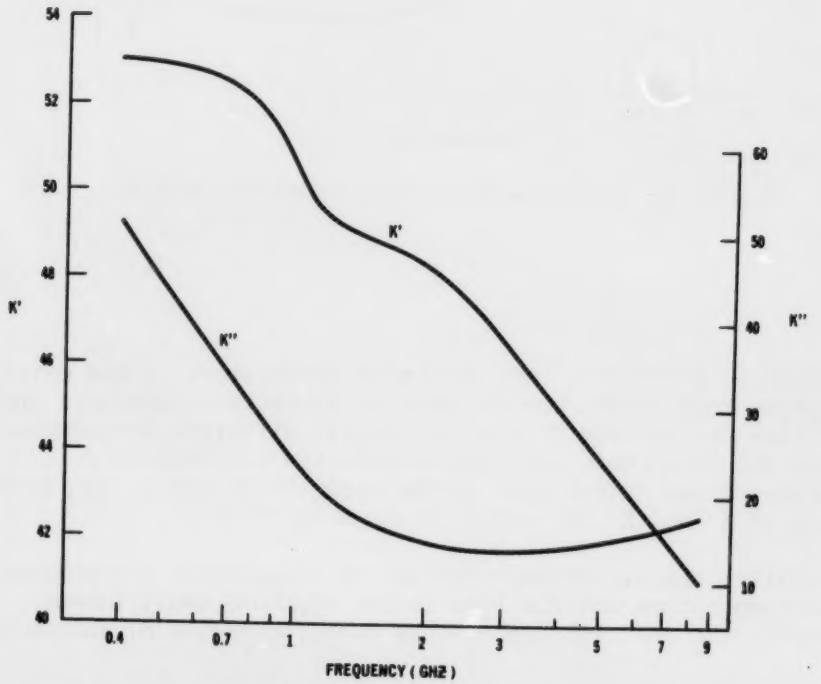

Figure 3C. Complex Dielectric Constant of Muscle.

TABLE 2. TEMPERATURE COEFFICIENT OF RELATIVE DIELECTRIC CONSTANT AND SPECIFIC RESISTANCE OF BODY TISSUES IN PERCENT PER DEGREE C[a]

Tissue	Frequency, MHz 50	200	1000
	$100 \frac{\Delta K'}{K'}$, °C		
Tissues with high H_2O content	0.5	0.2	-0.4
Fatty tissue	-	1.3	1.1
0.9% NaCl	-0.4	-0.4	-0.4
	$100 \frac{\Delta \rho}{\rho}$ °C		
Tissues with high H_2O content	-2	-1.8	-1.3
Fatty tissue	-(1.7 - 4.3)	-4.9	-4.2
0.9% NaCl	-2.0	-1.7	-1.3

[a]Taken from reference 16.

in living animals; therefore, in recognition of the normal variance in the measured dielectric paramenter values, temperature effects have been given no consideration here. Schwan discusses this particular aspect in more detail (11).

Various techniques for determining dielectric properties have been utilized; DC and low frequency AC fields are usually measured using bridge techniques while transmission line and waveguide approaches are used at ultrahigh frequencies. Descriptions of the application of these methods are abundant in the literature (20-24).

IMPEDANCE CALCULATIONS IN MULTI-LAYERED TISSUE SYSTEMS

Solutions to the field distributions within a multilayered tissue system are based on transmission line concepts. This approach requires knowledge of the electrical impedance of the various media involved.

In vacuum, or free space,

$$Z_o^* = \sqrt{\frac{\mu_o^*}{\epsilon_o^*}} = (377 + j0) \text{ ohms} \qquad \text{(Eq. 1)}$$

TABLE 3. DIELECTRIC PROPERTIES OF WATER AT SELECTED FREQUENCIES AND TEMPERATURES[a]

°C	Parameter	Frequency, MHz			
		300	3,000	10,000	25,000
1.5	K'	86.5	80.5	38.0	15.0
	K''	2.77	25.0	39.1	6.38
5	K'	85.2	80.2	41.0	17.5
	K''	2.33	22.1	39.0	6.91
15	K'	81.0	78.8	49.0	25.0
	K''	1.70	16.2	34.3	8.25
25	K'	77.5	76.7	55.0	34.0
	K''	1.24	12.0	29.7	9.01
35	K'	74.0	74.0	58.0	41.0
	K''	0.925	9.40	25.5	8.82
45	K'	71.0	70.7	59.0	46.0
	K''	0.746	7.49	23.6	12.7
55	K'	68.0	6.75	60.0	49.0
	K''	0.626	0.601	21.6	12.0
65	K'	64.5	64.0	59.0	50.5
	K''	0.542	4.90	18.9	6.31
75	K'	61.0	60.5	57.0	51.5
	K''	0.470	3.99	16.0	5.41
85	K'	57.0	56.5	54.0	-
	K''	0.416	3.09	14.0	-
95	K'	52.0	52.0	-	-
	K''	0.364	2.44	-	-

[a]Data taken from reference 35

where Z_o^* is the characteristic wave impedance of free space and μ_o^* and ε_o^* are as previously defined. In a material

$$Z_m^* = \sqrt{\frac{\mu_m^*}{\varepsilon_m^*}} \qquad \text{(Eq. 2)}$$

where Z_m^* is the characteristic wave impedance of the given material and μ_m^* and ε_m^* are the complex permeability and permittivity, respectively. If Eq. 2 is divided by Eq. 1,

$$\frac{Z_m^*}{Z_o^*} = \frac{\sqrt{\frac{\mu_m^*}{\varepsilon_m^*}}}{\sqrt{\frac{\mu_o^*}{\varepsilon_o^*}}}$$

As pointed out earlier, μ_m^* is set equal to μ_o^* in biological materials, and

$$Z_m^* = Z_o^* \sqrt{\frac{\varepsilon_o^*}{\varepsilon_m^*}} = Z_o^* \sqrt{1/K_m^*} = \frac{Z_o^*}{\sqrt{K_m^*}} \qquad \text{(Eq. 3)}$$

If the modulus or magnitude of the wave impedance for the material is needed, the modulus $|K_m^*|$ is used for the quantity under the radical sign, i.e.,

$$|Z_m^*| = \frac{Z_o}{\sqrt{\sqrt{K_m'^2 + K_m''^2}}}$$

where Z_o^* is written simply as Z_o since, in actuality, Z_o is purely real; the asterisk is used merely to emphasize that impedance, in general, is a complex quantity. It is convenient to express the intrinsic wave impedance of a medium (the subscript m refers to a given medium) in the familiar form

$$Z_m^* = R_m + jX_m \qquad \text{(Eq. 4)}$$

where R_m represents the resistive component of Z_m^*, and X_m represents the reactive component of Z_m^* as illustrated in Fig. 4. Equation 3 may be manipulated as follows:

$$Z_m^* = \frac{Z_o}{\sqrt{K_m^*}} = \frac{Z_o}{\sqrt{K_m' - jK_m''}} \cdot \frac{\sqrt{K_m' + jK_m''}}{\sqrt{K_m' + jK_m''}} = \frac{Z_o \sqrt{K_m' + jK_m''}}{\sqrt{K_m'^2 + K_m''^2}}$$

$$= \frac{Z_o}{\sqrt{K_m'^2 + K_m''^2}} \cdot \sqrt{\sqrt{K_m'^2 + K_m''^2}\ \angle \delta = \tan^{-1} \frac{K_m''}{K_m'}}$$

$$= \frac{Z_o}{\sqrt{\sqrt{K_m'^2 + K_m''^2}}} \qquad \angle \theta = \frac{\delta}{2} = \frac{1}{2} \tan^{-1} \frac{K_m''}{K_m'}$$

The angle δ, or loss angle, and its tangent (known as the loss tangent) are depicted in Figure 5. From the foregoing the defining equations

$$R_m = |Z_m^*| \cos \theta; \qquad X_m = |Z_m^*| \sin \theta; \qquad \theta = \frac{1}{2} \tan^{-1} \frac{K_m''}{K_m'}$$

may be used to express the intrinsic wave impedance of a material. This representation may be readily applied to the Smith diagram to solve various impedance transformation problems related to the slab tissue model (10). However, before the graphic-analytic technique of solution is described, it is necessary to define a few more quantities related to electromagnetic energy absorption in a material.

Whenever an electromagnetic wave is propagated in a given medium, the wave is both attenuated in amplitude and changed in phase; that is, the wave energy is absorbed within the medium and the wave velocity is altered. The electric field component of a wave propagated in a dielectric medium varies according to

$$E = E_o e^{-\gamma^* x} \qquad \text{(Eq. 5)}$$

where E is the field strength value at distance x in the medium, and E_o is the initial field strength at x = 0. Thus, it is appropriate to describe the wave propagation constant γ^* which is

a complex factor composed of the linear attenuation factor α (units of reciprocal length) and the phase factor β (measured in radians per unit length) where

$$\gamma^* = \alpha + j\beta = j\omega\sqrt{\varepsilon^* \mu^*}$$

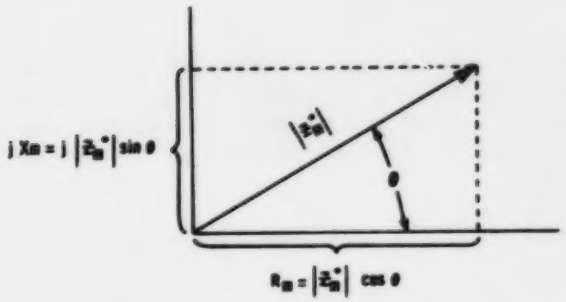

Figure 4. Vector Representation of Z_m^*.

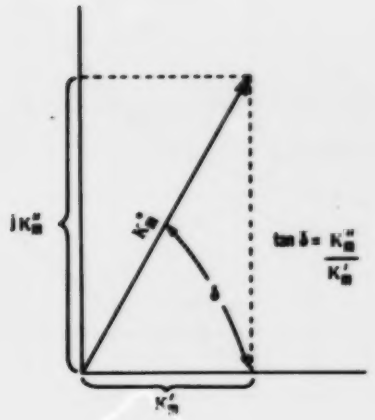

Figure 5. Vector Representation of K_m^*.

Expressions for α and β will not be derived here but only the formulas stated:

$$\alpha = \frac{2\pi}{\lambda_o} \sqrt{\frac{K'_m}{2}\left(\sqrt{1 + \tan^2 \delta} - 1\right)} \qquad \text{(Eq. 6)}$$

$$\beta = \frac{2\pi}{\lambda_o} \sqrt{\frac{K'_m}{2}\left(\sqrt{1 + \tan^2 \delta} + 1\right)} \qquad \text{(Eq. 7)}$$

where λ_o is the free space (vacuum) wavelength of the wave and $\tan \delta = K''_m/K'_m$. The unit of length used for λ_o determines the units for α and β. Values of α and β have been calculated, based on the dielectric data in Table 1, and are plotted as a function of frequency in Fig. 6.

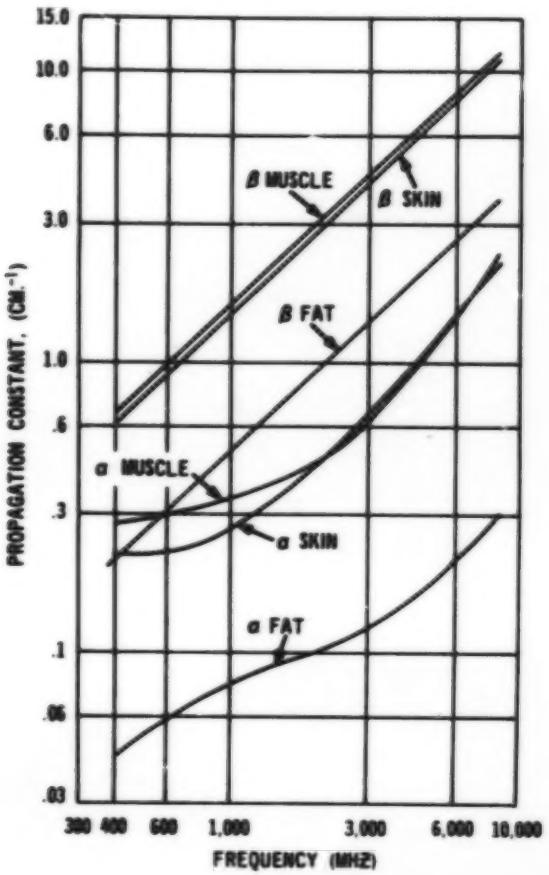

Figure 6. Propagation Constant of Skin, Fat, and Muscle.

Occasionally, a slightly different form for α is used when dielectric data are given in terms of K' and ρ (resistivity) rather than K' and K''. This expression takes the form

$$\alpha = \frac{2\pi}{\lambda_o} \sqrt{\frac{K'_m}{2}\left[\sqrt{1 + \left(\frac{60\lambda_o}{K'_m \rho}\right)^2} - 1\right]} \qquad \text{(Eq. 8)}$$

Here ρ must be in units of ohm-cm and λ_o in units of cm. Appendix A verifies the identity

$$\tan \delta = \frac{60\lambda_o}{K'_m \rho}$$

From the expression for the phase factor β, the wavelength of an EM wave (λ_m) with freespace wavelength λ_o, in a given material can be computed as

$$\lambda_m = \frac{2\pi}{\beta} = \frac{\lambda_o}{\sqrt{\frac{K'_m}{2}\left[\sqrt{1 + \tan^2 \delta} + 1\right]}}$$

Appendix B gives the derivation of another, equivalent expression for wavelength reduction in a dielectric material.

TOTAL DOSE ABSORBED BY SYSTEM

To calculate the total energy deposited in any infinite slab dielectric system by a plane wave, the reflection coefficient Γ^* must be determined for the exterior surface of the system. $|\Gamma^*|$ is defined as the ratio of the amplitude of the reflected EM wave to the amplitude of the incident wave; specifically, $|\Gamma^*|$ is related to the amplitudes of the electrical field (voltage) components of the EM waves and consequently, when squared, $|\Gamma^*|^2$ refers to the power reflected at a given interface. Once Γ^* is determined, the total energy or power extracted from an impinging EM wave may be computed for the total system. At this point only total deposited energy or power is computed; its distribution throughout the system is not specified.

For the slab model system considered here, assuming the base layer to be infinite in depth, the surface area for impinging waves semi-infinite in extent, and plane wave propagation, it can

be shown that the impedance at any point p through the tissue system is given by

$$Z_p^* = Z_c^* \frac{Z_L^* \cosh \gamma d + Z_c^* \sinh \gamma d}{Z_c^* \cosh \gamma d + Z_L^* \sinh \gamma d} \qquad \text{(Eq. 9)}$$

Z_c^* refers to the complex characteristic, or intrinsic impedance of the material containing the point p, and Z_L^* is the complex effective load impedance resulting from the discontinuity with underlying layers for the propagating wave. γ is the propagation constant for the material containing point p and d is the distance of point p from the interface defining Z_L^*. A stepwise process is used for systems composed of more than one material starting at the interface lying deepest and working outward toward the surface; each layer of material successively becomes the load, with a corresponding effective load impedance, for the next adjacent medium. In this method, the surface impedance at the air-tissue interface is finally determined from which Γ^* may be computed as

$$\Gamma^* = \frac{Z^* \text{ (surface)} - Z_o}{Z^* \text{ (surface)} + Z_o} \qquad \text{(Eq. 10)}$$

Subsequently, the percentage power absorbed by the system, $1 - |\Gamma^*|^2$ can be obtained.

Because of the inherent complexity of computation for this procedure, a simplified technique utilizing the Smith chart can be used to evaluate surface reflection coefficients. A brief description of this method, by way of an example, is useful before details are given concerning the computer generated solutions of Equations 9 and 10 as applied to some tissue systems.

As an example of the Smith chart technique of determining surface reflection consider a model system composed of 3 cm of fat tissue and 0.2 cm of skin tissue arranged over a semi-infinite layer of muscle tissue exposed to EM energy at a frequency of 2450 MHz. The model configuration is shown in Fig. 7 with material parameters indicated.

The first step involves making a table of derived parameters for the various tissues. Table 4 gives this information for the model under consideration.

TABLE 4. PARAMETERS FOR TISSUES IN FIGURE 7

Tissue	K'	K''	$\lvert Z^*_m \rvert$	R (ohm)	X (ohm)	θ (deg.)	λ_m (cm)	α_m (cm^{-1})
Skin	42.9	14.0	56.1	55.4	8.82	9.05	1.85	0.541
Fat	5.83	1.01	155.0	154.4	13.3	4.92	5.05	0.107
Muscle	47.6	13.7	53.6	53.1	7.51	8.05	1.76	0.504

Values for normalized impedance will be plotted for each numbered point which is indicated in Fig. 7. For the first point, point 2, the load impedance at the interface is represented by the intrinsic wave impedance for muscle since it is assumed that no waves entering the muscle are reflected. This load impedance, Z^*_M, must be normalized with respect to the wave impedance of fat in order to be plotted on the Smith chart and is determined as

$$\lvert Z^*_2 \rvert = \frac{\lvert Z^*_M \rvert}{\lvert Z^*_F \rvert} = \frac{53.6}{155.0} = 0.346$$

The phase angle of Z^*_2 is $\phi_2 = \theta_M - \theta_F = 8.05^o - 4.92^o = 3.13^o$. R then is $\lvert Z^*_2 \rvert \cos 3.13^o$ and X_2 is $\lvert Z^* \rvert \sin 3.13^o$. Z^*_2 may now be plotted at $Z^*_2 = 0.345 + j\ 0.0189$ (see Fig. 8). Now, the thickness of fat, 3.0 cm, is expressed in terms of the wavelength for 2450 MHz waves in fat tissue. 3.0 cm is found to be 0.594 λ_F and point 2 on the chart is rotated in a clockwise manner until 0.594 wavelengths have been passed. Since one full revolution on the Smith chart represents one-half wavelength, the new point is located at an angular displacement equivalent to a reading of 0.597 wavelengths toward the generator, allowing for an initial displacement of approximately 0.003 for point 2. A circle of constant voltage standing wave ratio (VSWR) is scribed about the origin for the appropriate degree of shift.

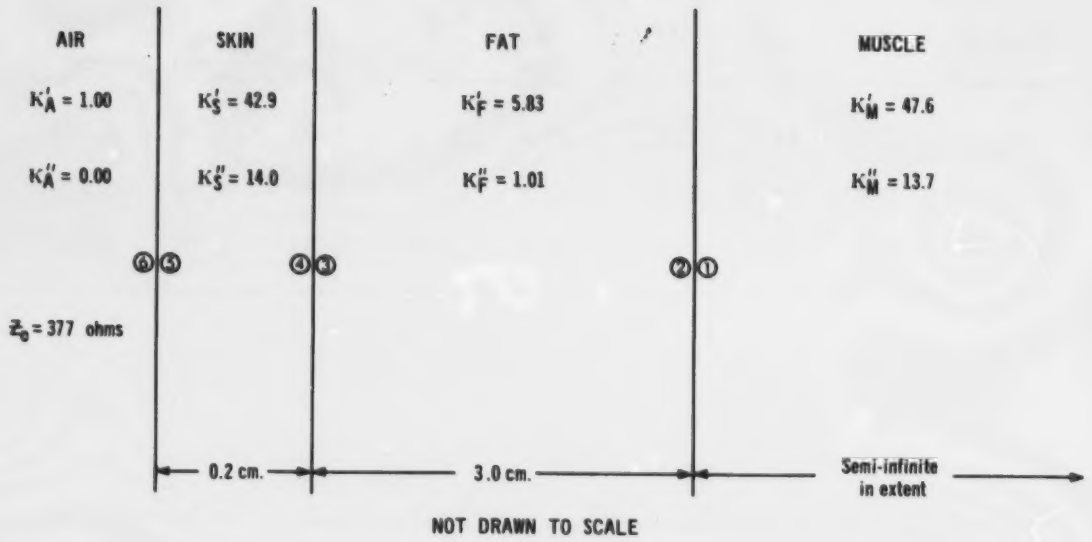

Figure 7. Model Configuration for Smith Chart Solution.

The radius is reduced by an amount equal to

$$e^{-2\alpha_F x_F} = e^{(-2)(0.107)(3.0\ \text{cm})} = 0.526$$

of its initial length. This completes the plotting of point 3 on the chart as $Z_3^* = 0.75 + j\ 0.38$. To go from point 3 to point 4, the modulus and phase angle for Z_4^* are computed again separately. A notation is made that the phase angle for Z_3^* is $\phi_3 = \tan^{-1}(0.38/0.75) = 26.9^o$

The modulus $|Z_4^*|$, normalized with respect to skin, is computed as

$$|Z_4^*| = \frac{|Z_3^*|\ |Z_F^*|}{|Z_S^*|} = 2.32 \text{ ohms}$$

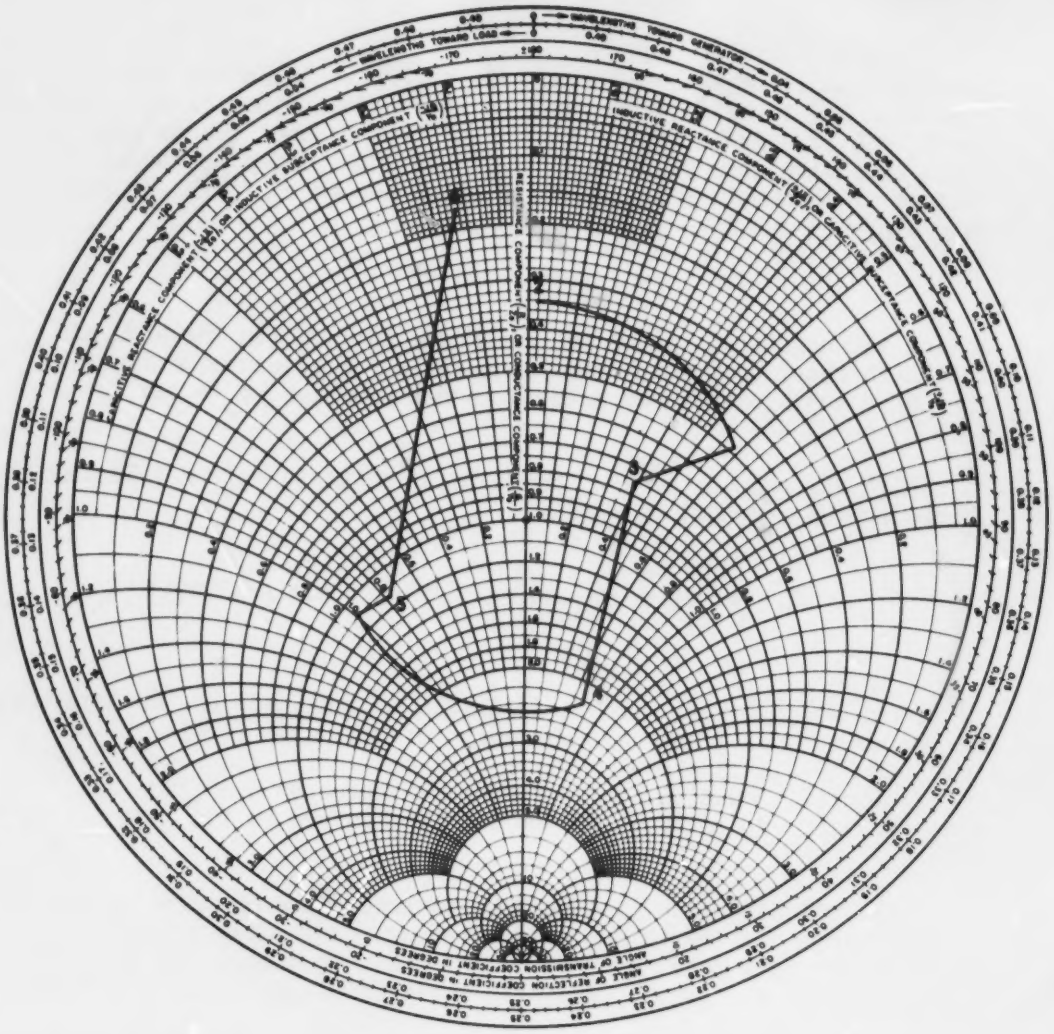

Figure 8. Smith Chart Solution. Chart grid reproduced by permission of Phillip H. Smith. Copyrighted 1949 and 1966 by Kay Electric Company, Pine Brook, N. J.

The phase angle of Z_4^* is $\phi_4 = \phi_3 - \theta_S = 17.8^o$. As before the resistive and reactive components of Z_4^* are determined as $R_4 = 2.21$ and $X_4 = 0.71$. Again, point 4 must be rotated about the origin equal to a displacement of 0.2 cm/1.85 λ_s and reduced in radius because of attenuation in the skin, by an emount $e^{-0.216} = 0.806$ This yields point 5 on the diagram located at

$$Z_5^* = 1.15 - j\ 0.77$$

Notice the negative sign of the imaginary part due to the side of the Smith chart upon which the point falls. Note consequently that the phase angle associated with Z_5^* is now negative, $\phi_5 = \tan^{-1}(-.670) = -33.8^o$.

With the modulus of the impedance at point 5, $|Z_5^*| = 1.38$, and Z_6^* may now be computed as,

$$Z_6^* = \frac{|Z_5^*|\ |Z_5^*|}{Z_o} [\cos(-33.8^o) + j \sin(-33.8^o)]$$

$|\Gamma^*|$, the voltage reflection coefficient modulus, may now be determined as the fractional length of the radius of the outer circle on the Smith chart. In this case, $|\Gamma^*| = 0.71$ and $|\Gamma^*|^2$, the power reflection coefficient is found to be .50 yielding a value of 0.50 for $1- |\Gamma^*|^2$, the percentage of incident power that is absorbed by the slab tissue system.

The reflection coefficient and its respective phase angle may be determined directly from the diagram by reading the appropriate scale at the perimenter of the circle. This completes the detailed description of the graphic-analytic analysis of impedance transformations.

A more complete and exact analysis of the problem can be performed by programming the mathematical approach on a computer. Such a program designed to compute values of $1 - |\Gamma^*|^2$ for an N layer system of tissue slabs, each with a characteristic K' and K'', and thickness, at a given frequency, was written. The output format as plots in Figures 9, 10 and 11 illustrate how the percentage of incident power absorbed in the system varies as a function of skin and fat thickness at 915, 2450, and 8500 MHz respectively. The first two frequencies are of particular interest from a human exposure viewpoint because they are designated as medical and industrial frequencies which include the use of diathermy and microwave ovens.

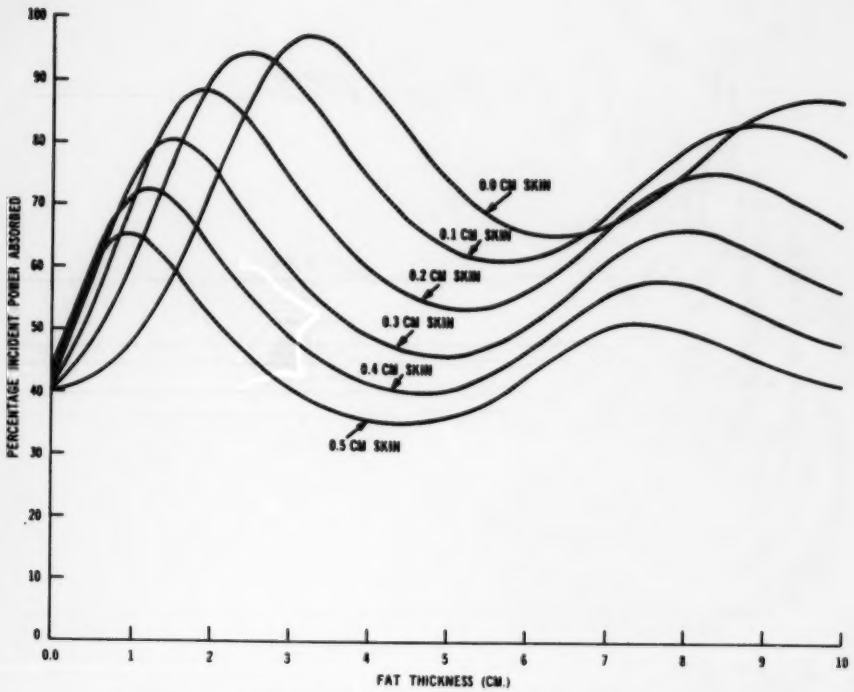

Figure 9. 915 MHz Power Absorption in Tissue.

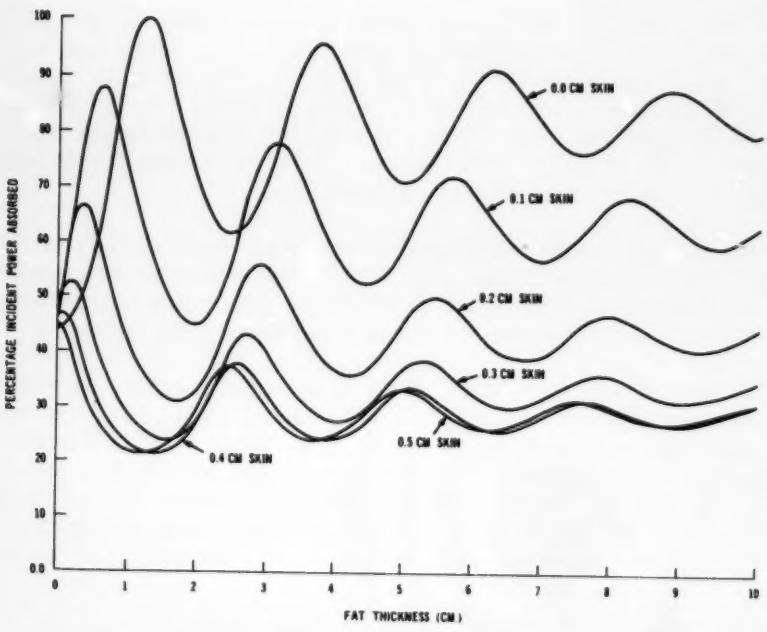

Figure 10. 2450 MHz Power Absorption in Tissue.

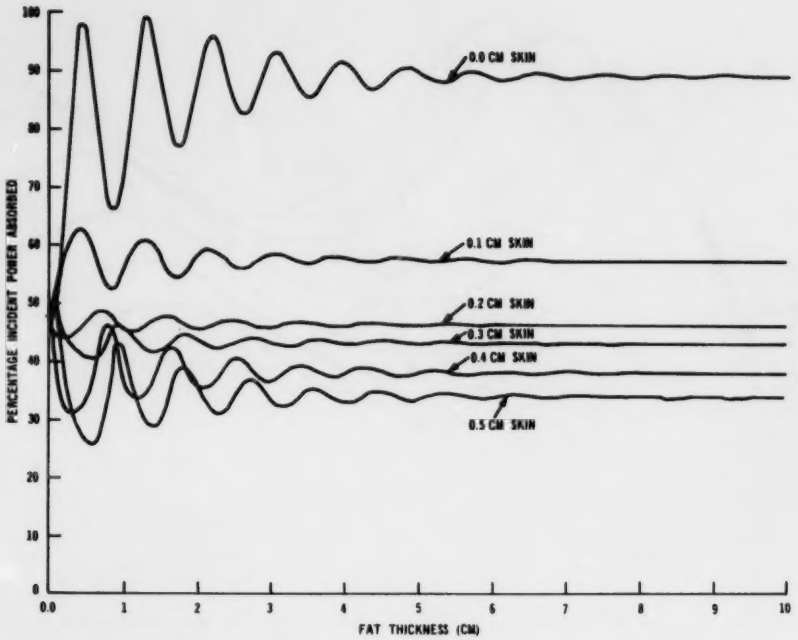

Figure 11. 8500 MHz Power Absorption in Tissue.

At 915 MHz, with up to 0.4 cm skin, the presence of fat tissue always increases the total amount of power which is absorbed by the system. The addition of skin to a fat muscle complex with fat dimensions greater than 3 cm generally decreases the percentage power absorbed, while at fat thicknesses less than 3.0 cm, the inclusion of skin to the model may enhance power absorption. This relationship is critically dependent on the particular tissue dimensions.

Over the entire range of tissue dimensions considered, which, in general, span the maximum range over which these dimensions would ever take in humans, at 915 MHz the absorbed power may vary between 35 and 97 percent, or by a factor of approximately three.

At 2450 MHz, the presence of skin is more effective in reducing the extent of total power absorption. In this case, the presence of fat tissue also increases absorption as long as the skin thickness is less than 0.1 cm, compared with 0.4 cm at 915 MHz. This occurs because skin tissue becomes markedly less transparent as the frequency is increased. The possible range in percentage power absorption by the model at 2450 MHz extends from about 21 to 100 percent, or a

factor of about five. As skin thickness exceeds 0.1 cm, power absorption at any given fat thickness greater than about 0.5 cm is generally reduced.

As the frequency is increased to 8500 MHz, the presence of skin is strikingly apparent. So long as the model is restricted to skin layers less than 0.2 cm, the presence of fat generally increases the amount of power absorbed. This time, for the range of possible dimensions considered, the power absorbed by the system may range from about 26 to 99 percent, or a factor of about four. Thus, 2450 MHz represents the frequency of EM energy, of the three frequencies considered, which provides the most variable degree of possible coupling between field and model.

All three figures are characterized by the appearance of periodic relative peaks in power absorption. These peaks occur at intervals of $\lambda F/2$ with the first peak of any curve for no skin appearing at a fat thickness equal to a quarter wavelength for the wave in fat at that frequency. In this respect it may be assumed that the fat is acting as a quarter-wave impedance transformer, optimizing the coupling of energy, or power, between air and the tissue slabs. Increasing the fat thickness illustrates the damping effect due to loss in the fat.

From these data and the given incident power density of a microwave exposure field, the coupling between a particular model configuration and the field may be established. The exact distribution of this absorbed power, as manifested in heat development, will next be traced through selected systems.

DOSE DISTRIBUTION WITHIN SYSTEM

In deriving the spatial distribution of heating in the slab model, the deepest lying interface is taken as the origin of coordinates upon which all calculations will be referenced. An effective incident wave, E_o, will be assumed. It is a composite of the sum of the initial wave transmitted directly from the radiation source and all positively directed reflections arising within the medium adjacent to the interface. As Schwan points out, the reflection coefficient for such a sum of waves can be shown to be identical with that for a single wave (9). All distances measured to the right of an interface are positive and distances to the left are negative.

For a skin-fat-muscle system, consider the electric field at any point within the fat material. Here the electrical field may be

expressed as the resultant of the incident and reflected waves.

$$E_{Fat} = E_{incident} + E_{reflected} = E_o\left(e^{-\gamma_F x} + \Gamma^*_{FM} e^{\gamma_F x}\right) \quad x < 0 \qquad \text{(Eq. 11)}$$

To arrive at an expression for the magnetic field, Maxwell's equation from Faraday's law,

$$\underset{\sim}{\nabla} \times \underset{\sim}{E} = -\frac{\partial \underset{\sim}{B}}{\partial t} = -\mu \frac{\partial \underset{\sim}{H}}{\partial t}$$

is expanded in rectangular coordinates.

$$\underset{\sim}{i}\left(\frac{\partial Ez}{\partial y} - \frac{\partial Ey}{\partial z}\right) + \underset{\sim}{j}\left(\frac{\partial Ex}{\partial z} - \frac{\partial Ez}{\partial x}\right) + \underset{\sim}{k}\left(\frac{\partial Ey}{\partial x} - \frac{\partial Ex}{\partial y}\right)$$

$$= -\mu \frac{\partial}{\partial t}\left(\underset{\sim}{i}Hx + \underset{\sim}{j}Hy + \underset{\sim}{k}Hz\right) \qquad \text{(Eq. 12)}$$

For a plane wave traveling in the x direction of the slab model, the only components of Eq. 12 which contribute are

$$\underset{\sim}{k}\frac{\partial Ey}{\partial x} = -\mu \underset{\sim}{k}\frac{\partial Hz}{\partial t}$$

or,

$$H = -\frac{1}{\mu}\int \frac{\partial E}{\partial x} dt$$

and when E varies in time according to $E = E_o e^{j\omega\tau}$,

$$H_{fat} = \frac{E_o \gamma_F}{j\mu_F \omega}\left(e^{-\gamma_F x} - \Gamma^*_{FM} e^{\gamma_F x}\right) \qquad x < 0 \qquad \text{(Eq. 13)}$$

where: Γ^*_{FM} = complex reflection coefficient at fat-muscle interface

γ_F = complex propagation constant for fat

μ_F = permeability of fat medium

ω = angular frequency of wave = $2\pi f$

The value of the E field transmitted into the muscle, at the interface is

$$E_{transmitted} = E_o\ (1 + \Gamma^*_{FM})$$

from equation 11 when x is zero. With this value of E just inside the muscle tissue, the description of the E and H fields anywhere in the muscle are obtained through a similar procedure as

$$E_{muscle} = (1 + \Gamma^*)\ E_o e^{-\gamma_M x} \qquad x > 0 \qquad \text{(Eq. 14)}$$

$$H_{muscle} = (1 + \Gamma^*)\ \frac{E_o \gamma_M}{j\mu_M \omega}\ e^{-\gamma_M x} \qquad x > 0 \qquad \text{(Eq. 15)}$$

For other layers of tissue, such as skin, which lie on top of the fat tissue, equations similar to Eq. 11 and Eq. 13 are obtained with appropriate substitution of dielectric parameters and a factor which corrects for the change in the E field which occurs as the origin of coordinates is moved to the left. The appropriate forms of these equations are:

$$E_{skin} = E_o e^{-\gamma_F d_F} (e^{-\gamma_S x_S} + \Gamma^*_{SF} e^{\gamma_S x_S}) \qquad \begin{matrix} x < 0 \\ d_F < 0 \end{matrix} \qquad \text{(Eq. 16)}$$

$$H_{skin} = E_o \frac{e^{-\gamma_F d_F}\ \gamma_S}{j\mu_S \omega} (e^{-\gamma_S x_S} - \Gamma^*_{SF} e^{\gamma_S x_S}) \qquad \begin{matrix} x < 0 \\ d_F < 0 \end{matrix} \qquad \text{(Eq. 17)}$$

The intensity of the wave configuration in the tissues, or energy flow, is given by the complex Poynting vector, $I = 1/2\ \underset{\sim}{E}\bar{\underset{\sim}{H}}$. The bar above the H signifies that the complex conjugate for the quantity is used. This relation is arrived at after considering the expression

$$\int_S \underset{\sim}{S} \cdot n\ da = \int_S (\underset{\sim}{E} \times \underset{\sim}{H}) \cdot n\ da$$

where $\underset{\sim}{S}$ = the Poynting vector = $\underset{\sim}{E} \times \underset{\sim}{H}$ (watts/m^2). Though this relation can be interpreted as the total flow of energy (intensity) through a closed surface at a point in the field, it cannot definitely be concluded that the intensity of energy flow at a point is $\underset{\sim}{S} = \underset{\sim}{E} \times \underset{\sim}{H}$; there could be added to this quantity any vector integrating to zero over a closed surface without affecting the total flow. Complete details of this expression and how the complex Poynting vector is related to the actual physical entities involved in heat production are given by Stratton (25), pages 132-137.

When $\gamma = \alpha + j\,\beta$ and $\Gamma^* = |\Gamma^*|\, e^{j\phi}$, the intensities in fat and muscle are found to be

$$I_{fat} = \frac{1}{2} E_F \bar{H}_F = \left[\frac{\beta_F + j\alpha_F}{2\mu_F \omega} E_o \bar{E}_o \right] \qquad x < 0 \qquad \text{(Eq. 18)}$$

$$\left[e^{-2\alpha_F x} - |\Gamma^*_{FM}|^2 \, e^{2\alpha_F x} + j2\, |\Gamma^*_{FM}| \sin(2\beta_F x + \phi_{FM}) \right]$$

$$I_{muscle} = \frac{1}{2} E_M \bar{H}_M = \left(\frac{\beta_M + j\alpha_M}{2\mu_M \omega} E_o \bar{E}_o \right) \qquad x > 0 \qquad \text{(Eq. 19)}$$

$$\left(1 + 2\, |\Gamma^*_{FM}| \cos \phi_{FM} + |\Gamma^*_{FM}|^2 \right) e^{-2\alpha_M x}$$

Heat development rate per unit volume is computed by taking the negative space rate of change of the real part of the expressions for intensity (25).

$$- \frac{\partial}{\partial x} \text{Re}\, I_{fat} = \frac{1}{2} \frac{2\alpha_F \beta_F}{\mu_F \omega} E_o^2 \left[e^{-2\alpha_F x} + |\Gamma^*_{FM}|^2 \, e^{2\alpha_F x} \right.$$

$$\left. + 2\, |\Gamma^*_{FM}| \cos (2\beta_F x + \phi_{FM}) \right]$$

Since

$$\alpha_F \beta_F = \frac{\mu_F \sigma_F \omega}{2}$$

(see Appendix C), this expression reduces to

$$HDR_{fat} = \frac{1}{2} \sigma_F E_o^2 \left[e^{-2\alpha_F x} + |\Gamma^*_{FM}|^2 e^{2\alpha_F x} \right. \qquad x \leq 0$$

$$\left. + 2|\Gamma^*_{FM}| \cos (2\beta_F x + \phi_{FM}) \right] \qquad \text{(Eq. 20)}$$

Taking the negative derivative of the intensity in muscle, and recalling that the electrical field must be continuous across the interface, yields

$$HDR_{muscle} = \frac{1}{2} \sigma_M E_o^2 \left(1 + |\Gamma^*_{FM}|^2 + 2|\Gamma^*_{FM}| \cos \phi_{FM} \right) e^{-2\alpha_M x} \qquad \text{(Eq. 21)}$$

$$x > 0$$

where the term HDR refers to heat development rate.

Since, as pointed out, expressions for the E and H fields in any other tissue layers exterior to the two base layers (muscle and fat in this case) have forms such as Eqs. 16 and 17, formulas similar to Eq. 20 giving the heat development rate in other overlying tissues are obtained. In the case of a layer of skin tissue over the fat layer,

$$HDR_{skin} = \frac{1}{2} \sigma_S E_o^2 e^{-2\alpha_F d_F} \left[e^{-2\alpha_S x} + |\Gamma^*_{SF}|^2 e^{2\alpha_S x} \right. \qquad \text{(Eq. 22)}$$

$$\left. + 2|\Gamma^*_{SF}| \cos(2\beta_S x + \phi_{SF}) \right] \qquad x \leq 0$$

$$d_F < 0$$

Recall that as the distribution is worked out for each layer of tissue, starting with the deepest lying interface, the origin of coordinates is shifted to the left (in the model configuration) so that it defines the next considered interface. The sign convention for positive distances to the right and negative distances to the left of the interface is maintained. In this fashion, any number of tissue layers may be modeled and analyzed.

When only two layers of tissue are being considered, the heat development rates obtained are directly comparable. This is because a reference field, E_0, was established at the fat muscle interface and all expressions for intensity or HDR, in muscle or fat, were derived in terms of distance from this reference field. However, as additional layers are added to the model, and the origin of coordinates for deriving intensity and HDR in those layers is moved to the left, i.e., toward the source of radiation, the electrical field at this new interface must be written in terms of the reference field at the muscle-fat interface. This requires compensation for

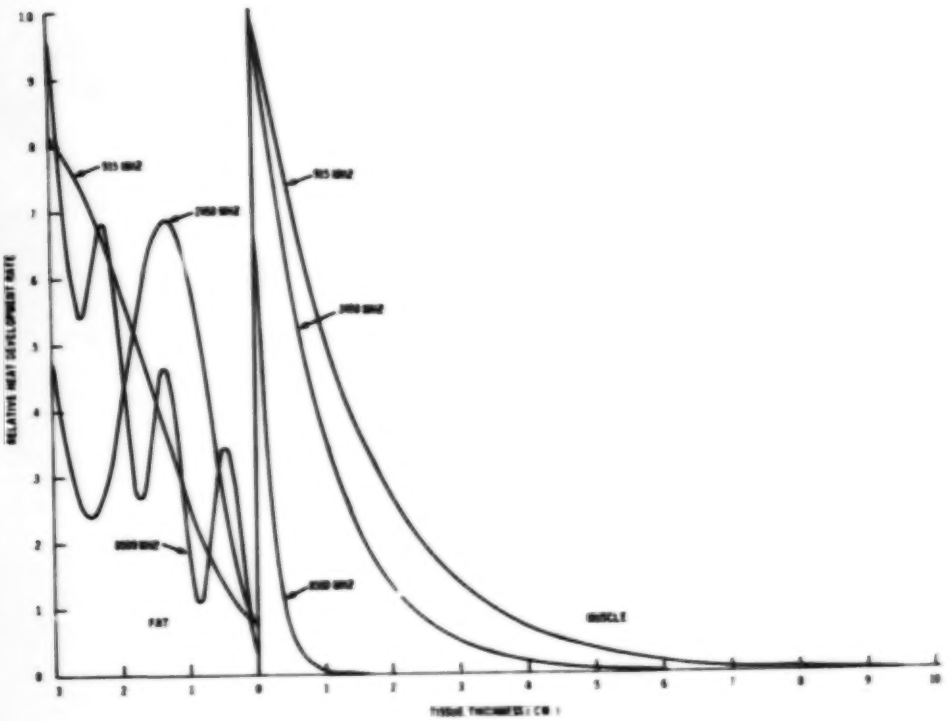

Figure 12. Relative Heat Development Rate in Two-Layer Model.

attenuation of the effective incident wave in the fat layer or multiplication by a factor of $e^{-\gamma_P d_F}$, $d < 0$. In the heat development formula, the correction term appears as $e^{-2\gamma_P d_F}$, having been squared in the process. This correction must be performed for all layers other than the two base layers, taking into account the attenuation occurring through all layers separating the new origin from the initial interface.

Figure 12 shows the relative heat development rate in the fat-muscle model at three different frequencies for a fixed fat thickness of 3 cm. The abrupt rise just inside the muscle layer is characteristic of the radical change in conductivity of the medium compared to that of fat. Relative peaks in the heating rate may be seen for frequencies high enough for standing wave formation to occur within the fat layer; the first peak in such cases always occurs a quarter wavelength in front of the reflective interface. This corresponds, in fat, to approximately 0.5 cm and 1.3 cm at 8500 and 2450 MHz, respectively. At 915 MHz, 3.0 cm of fat is not quite equal to a quarter wavelength so that the turning point of the first peak is not visible. At 2450 MHz surface heating of the fat layer is about 68 percent of the maximum heating which occurs deeper within the fat; the greatest rate of heat development in the entire model at this frequency occurs on the exterior-most surface of the muscle. At 915 MHz and 8500 MHz, surface heating of the fat layer predominates over the heating rate anywhere else in the medium.

Figure 13 illustrates the spatial distribution of the heat development rate for a three component system (0.2 cm skin, 3.0 cm fat and semi-infinite muscle) at 2450 MHz. In this diagram the scale for the skin thickness has been expanded by a factor of 10 to permit careful visual inspection of the heating distribution. Because 0.2 cm represents substantially less than a quarter wavelength in skin at even 8500 MHz, no oscillation of the heating rate from the standing wave pattern is seen. Skin heating is the obvious manifestation of microwave exposure for this model configuration at the higher frequencies. This follows from the fact that skin tissue becomes more lossy as the frequency is increased.

In summary, in slab tissue models with muscle as a base, tissue heating, on the average, tends to increase as the model is transversed axially from the deepest lying interface toward the exterior.

It is valuable to know the total quantity of heat developed within each of the layers of the model so that comparisons can be made as to which of the tissues receives the greatest thermal burden from exposure. This may be accomplished by integrating each of the expressions for heat development rates over the dimensions for the respective tissue slabs. The percentages of total heat developed in each tissue may then be plotted as a function of any tissue

dimension. In the case here, the subcutaneous fat layer thickness has been selected as the parameter to plot on the absicissa.

Expressions for the particular integrals of the HDR's (Eqs. 20, 21, 22) over total thicknesses d_i are obtained upon integration as:

$$\int_0^{d_M} HDR_M = \frac{\sigma_M E_o^2}{2\alpha_M}\left(1 + |\Gamma^*_{FM}|^2 + 2|\Gamma^*_{FM}|\cos\phi_{FM}\right)\left(\frac{1 - e^{-2\alpha_M d_M}}{2}\right) \qquad d_M > 0$$

$$\int_{d_F}^{0} HDR_F = \frac{\sigma_F E_o^2}{2}\left\{\frac{1}{2\alpha_F}\left[-1 + e^{-2\alpha_F d_F} + |\Gamma^*_{FM}|^2 - |\Gamma^*_{FM}|^2 e^{2\alpha_F d_F}\right]\right. \qquad d_F < 0$$

$$\left. + \frac{|\Gamma^*_{FM}|}{\beta_F}\left[\sin\phi_{FM} - \sin(2\beta_F d_F + \phi_{FM})\right]\right\}$$

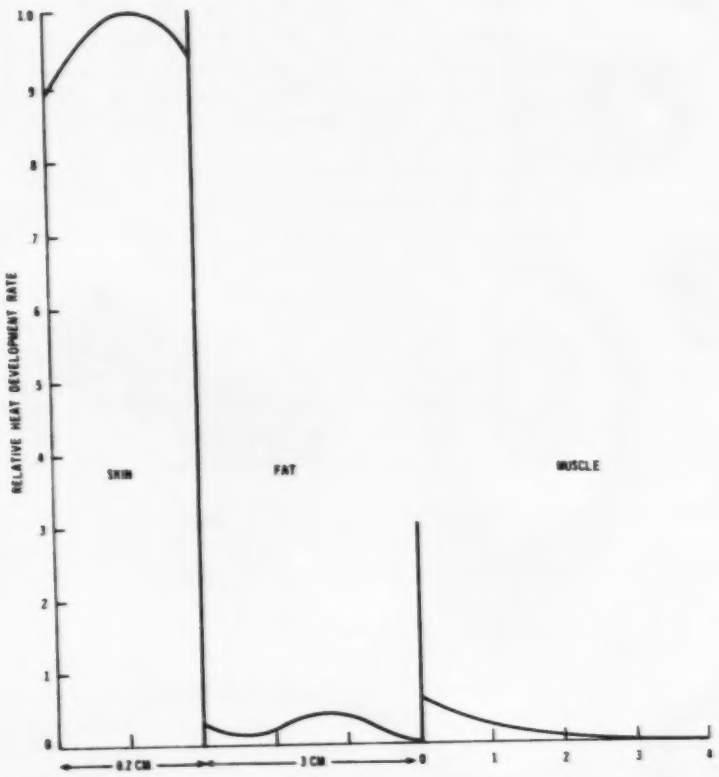

Figure 13. Relative Heat Development Rate in Three-Layer Model. Frequency is 2450 MHz.

$$\int_{d_S}^{0} HDR_S = \frac{\sigma_S E_0^2}{2} e^{-2\alpha_F d_F} \left\{ \frac{1}{2\alpha_S} \left[-1 + e^{-2\alpha_S d_S} + |\Gamma^*_{SF}|^2 - |\Gamma^*_{SF}|^2 e^{2\alpha_S d_S} \right] + \frac{|\Gamma^*_{SF}|}{\beta_S} \left[\sin \phi_{SF} - \sin(2\beta_S d_S + \phi_{SF}) \right] \right\} \qquad d_S < 0,\ d_F < 0$$

The sign convention for the thickness d is the same as before, muscle thickness being positive and fat and skin thicknesses (or any other tissue layers exterior to the deepest interface) being negative. Since the integral of heat development in skin has been normalized with respect the remainder of the layers, because of the correction factor $e^{-2\gamma_F d_F}$, the percentages of total heat developed may be displayed by plotting

$$\frac{\int HDR_M}{\int HDR_M + \int HDR_F}$$

as a function of d_F for a two component system. When skin, or a three or more component system is used,

$$\frac{\int HDR_M}{\int HDR_M + \int HDR_F + \int HDR_S}$$

is first plotted against d_F and then

$$\frac{\int HDR_M + \int HDR_F}{\int HDR_M + \int HDR_F + \int HDR_S}$$

is plotted on the same graph against d_F. Figures 14, 15, and 16 illustrate the results of such computations for two and three component systems. Where skin tissue is present, its thickness is varied to show the change in partition of heat development between the three tissues. By observing the various ordinate values of the curves at any particular fat thickness, the breakdown in total heat developed within the specified model may be determined. Total heat developed within the system is assigned a value of 100 percent.

In general, the curves illustrate that at the lower frequency, deep heating of the muscular tissue is more predominate while at the higher frequency, the heating of surface tissue is greater. Also, as Schwan discusses (11) the frequency range of approximately 1000 to 3000 MHz represents a range in which both the distribution of total incident energy absorbed by the model, and the development of heat in the various tissues are highly variable. That is, there is a transition zone, in terms of frequency, which more or less connects the regions showing deep heating at low frequencies and surface heating at higher frequencies. It is of interest from the

standpoint of public exposure to microwaves that the industrial-medical frequency of 2450 MHz lies in this complicated interaction region. The exact fraction of total heat developed within the various tissues is a function of an infinite set of possible tissue dimension combinations. Maximum values of fractional heating may be determined, however, for every possible combination within specified limits of the dimensions. If, for practical purposes, one considers skin thickness to vary from 0 to 3 mm, and the fat layer to vary between 0 and 4 cm, the following maximum values are obtained:

915 MHz

Maximum possible fractional skin heating = 60 percent
Maximum possible fractional fat heating = 29 percent

2450 MHz

Maximum possible fractional skin heating = 74 percent
Maximum possible fractional fat heating = 25 percent

8500 MHz

Maximum possible fractional skin heating = 93 percent
Maximum possible fractional fat heating = 9 percent

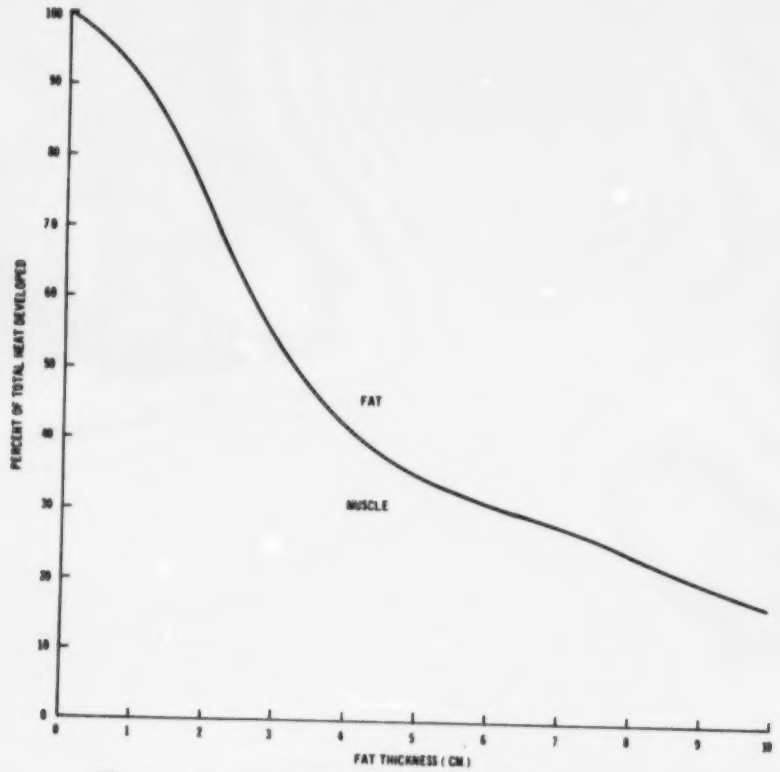

Figure 14A. Thermal Dose Distribution in Two-Component System at 915 MHz.

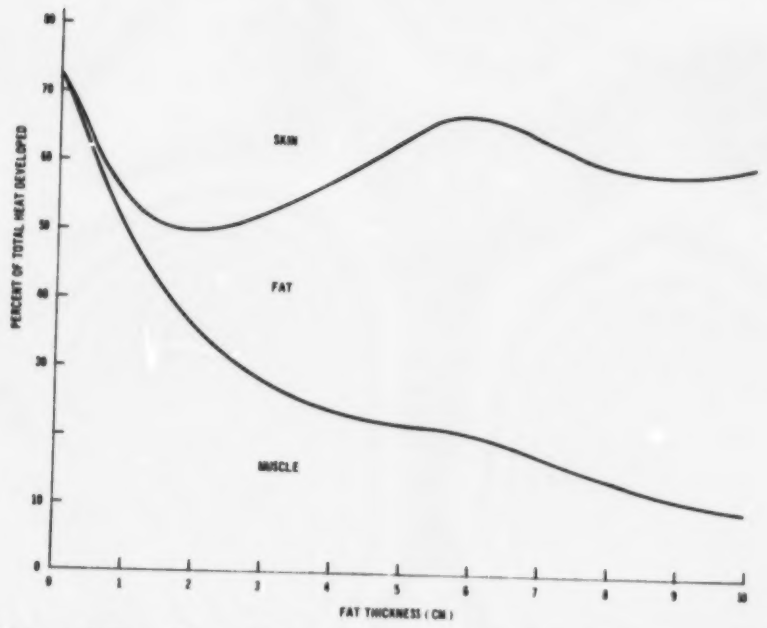

Figure 14B. Thermal Dose Distribution in Three-Component System at 915 MHz; Skin Thickness, 0.2 cm.

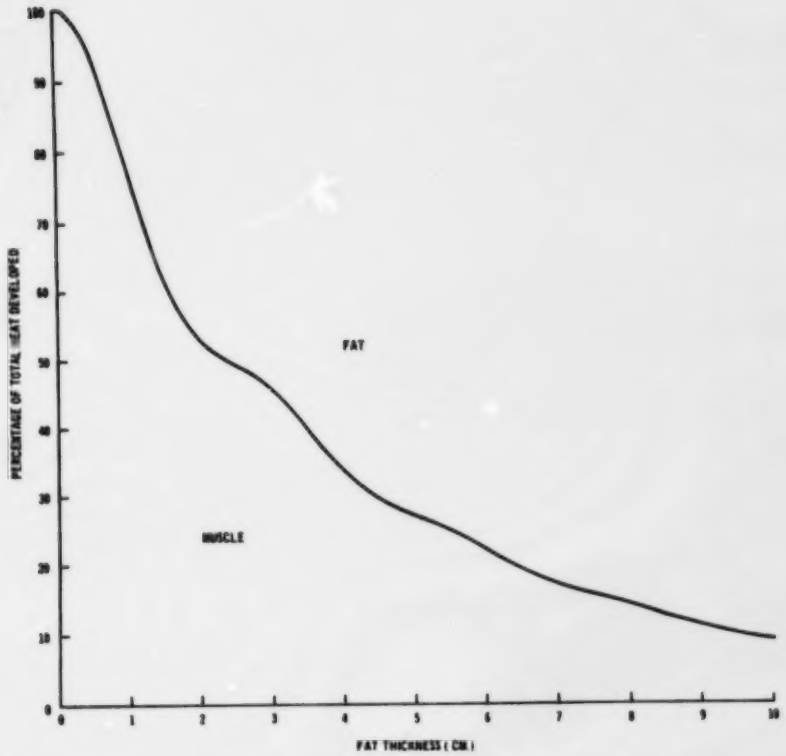

Figure 15A. Thermal Dose Distribution in Two-Component System at 2450 MHz.

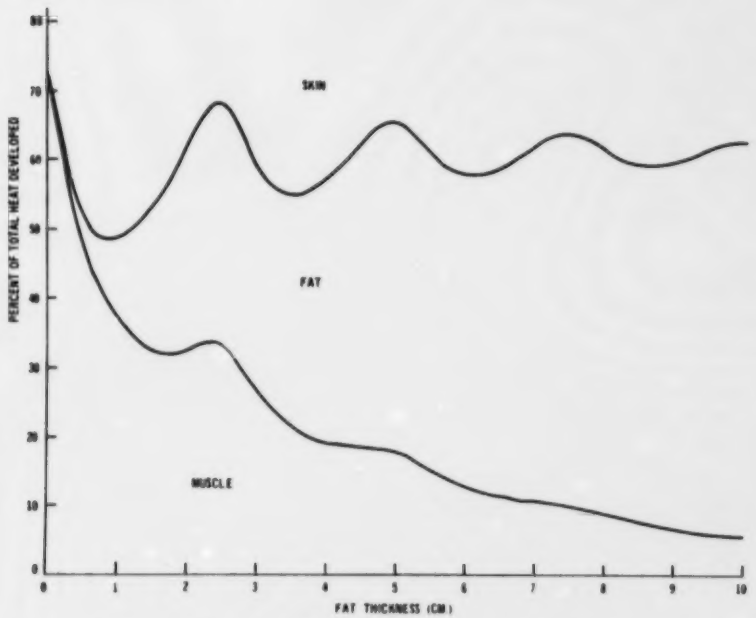

Figure 15B. Thermal Dose Distribution in Three-Component System at 2450 MHz; Skin Thickness, 0.1 cm.

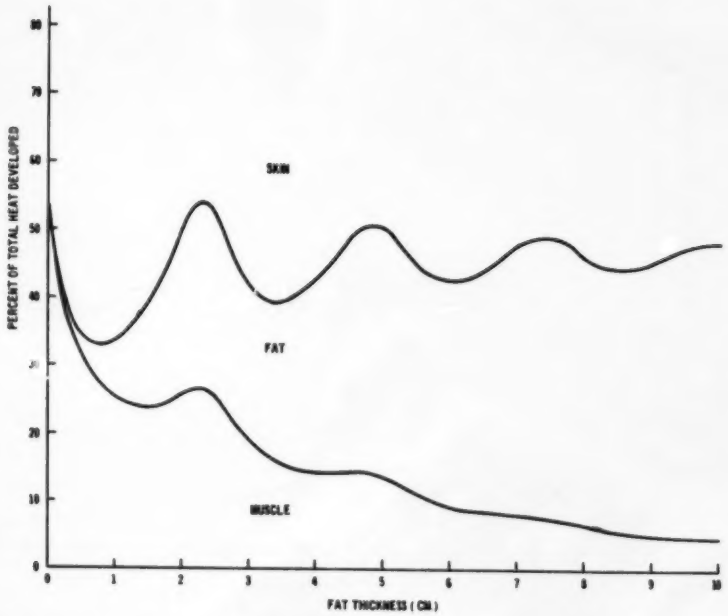

Figure 15C. Thermal Dose Distribution in Three-Component System at 2450 MHz; Skin Thickness, 0.2 cm.

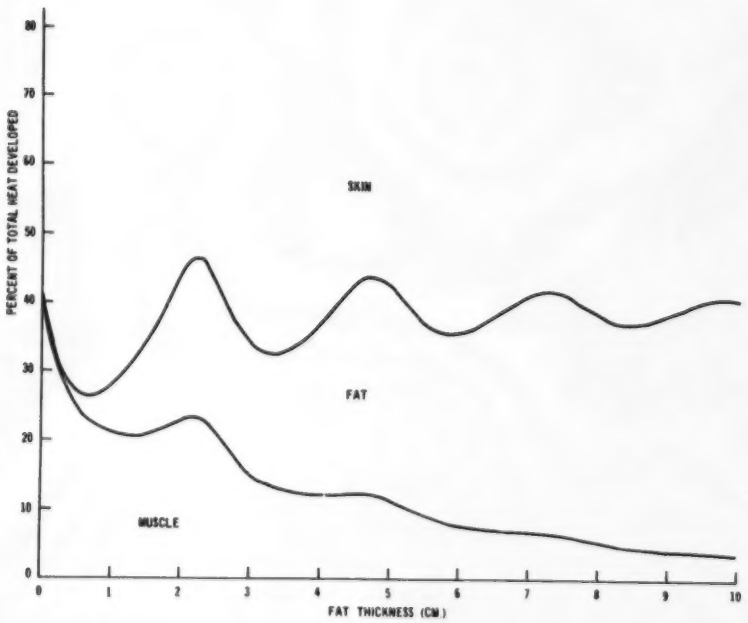

Figure 15D. Thermal Dose Distribution in Three-Component System at 2450 MHz; Skin Thickness, 0.3 cm.

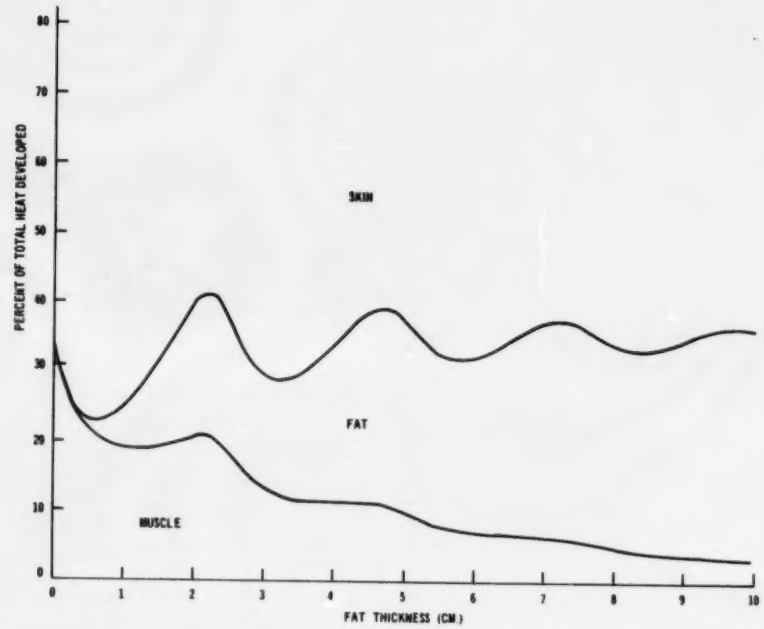

Figure 15E. Thermal Dose Distribution in Three-Component System at 2450 MHz; Skin Thickness, 0.4 cm.

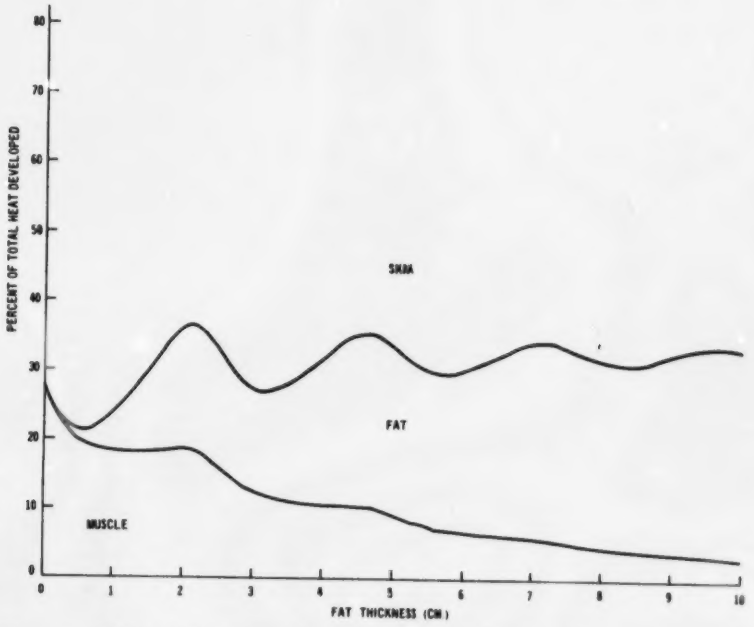

Figure 15F. Thermal Dose Distribution in Three-Component System at 2450 MHz; Skin Thickness, 0.5 cm.

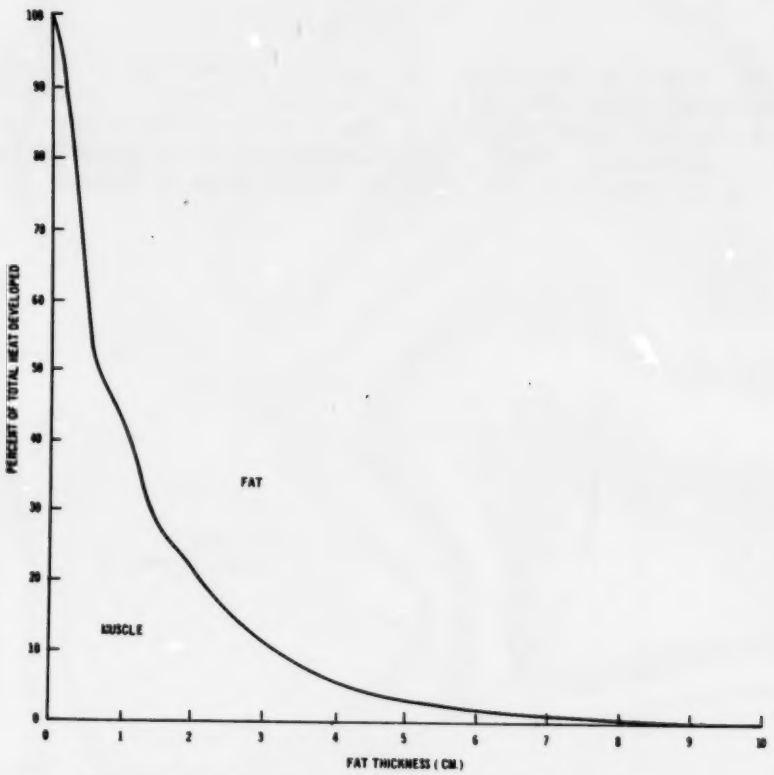

Figure 16A. Thermal Dose Distribution in Two-Component System at 8500 MHz.

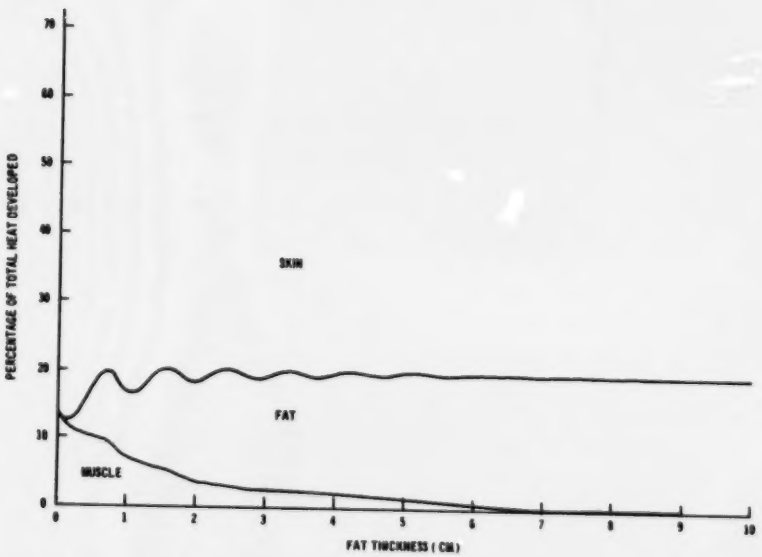

Figure 16B. Thermal Dose Distribution in Three-Component System at 8500 MHz; Skin Thickness 0.2 cm.

As skin thickness is increased the amount, percentage wise, of total heat developed within the skin layer becomes larger. Consequently, for any given fat layer dimension, the fractional heat developed within fat decreases. This general relationship is graphically illustrated in Figure 17 for 2450 MHz and 2.0 cm of fat.

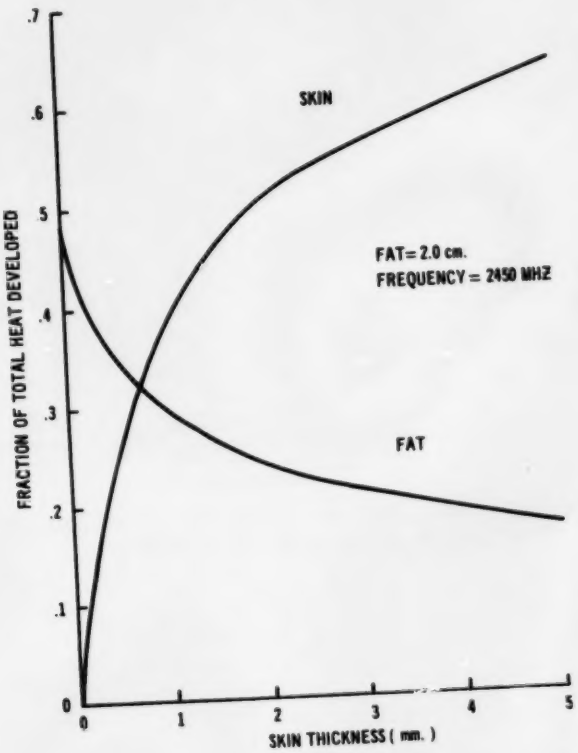

Figure 17. Effect of Skin Thickness on Fraction of Total Heat Developed in Skin and Fat.

COMMENTS ON TEMPERATURE RISE IN TISSUES

To evaluate the extent of temperature rise in the individual tissues it is necessary first to determine the percentage of incident power absorbed by the model, as from Figure 9, 10, or 11 (page 21). Once this quantity is known, the location of this power as heat generated can be determined as from Figures 14, 15, 16 (page 33). From the amount of power (watts) delivered to each layer of tissue, the period of exposure, the initial temperature of the particular tissue, and the specific heat capacity of the tissue, one can estimate the final temperature of the medium. This estimation does not take into account blood circulation in the model; radiation, convection, or conduction of heat to the ambient environment; nor does it hold when such low intensities of exposure are used that heat flow within the model is significant (i.e., the time of exposure is long compared with the time constants which characterize heat exchange in the model). The effects of radiation, evaporation of perspiration, or conduction such as would occur in an animal are also not considered. Thus, under these restricted conditions, where for a transient period of time the tissue temperature rise is linear with time of exposure, an attempt can be made to estimate what might be called a total microwave thermal dose delivered to the model (a product of exposure time and absorbed energy flux).

The use of such information to propose standards or limits for human exposure to microwaves, however, should be made carefully because of the obvious variables and assumptions involved. Specifying the maximum tolerance dose (watt-min/cm^2) for humans must incorporate biological studies to determine what tissue temperatures are allowable for any exposure time. A corresponding study must be done to find what tissue temperature elevation rates are associated with these maximum allowable tissue or body temperatures.

Several studies have been reported that deal with the effects of heat stress in humans (26, 27). These data, as applied to the case of microwave heating, have been used to illustrate the necessity of lowering exposure limits in other than ideal environmental circumstances (28). However, in light of the restrictions imposed, it is still possible to examine the thermal load placed on various tissues in the model system. These estimates provide a means of visualizing, in an approximate manner, the heating that will occur in living tissue systems of humans.

Thermal loads in various layers of the stratified model tissue system may be evaluated in terms of maximum temperature excursions during the irradiation time. In general the thermal energy imparted

COMMENTS ON TEMPERATURE RISE IN TISSUES

To evaluate the extent of temperature rise in the individual tissues it is necessary first to determine the percentage of incident power absorbed by the model, as from Figure 9, 10, or 11 (page 21). Once this quantity is known, the location of this power as heat generated can be determined as from Figures 14, 15, 16 (page 33). From the amount of power (watts) delivered to each layer of tissue, the period of exposure, the initial temperature of the particular tissue, and the specific heat capacity of the tissue, one can estimate the final temperature of the medium. This estimation does not take into account blood circulation in the model; radiation, convection, or conduction of heat to the ambient environment; nor does it hold when such low intensities of exposure are used that heat flow within the model is significant (i.e., the time of exposure is long compared with the time constants which characterize heat exchange in the model). The effects of radiation, evaporation of perspiration, or conduction such as would occur in an animal are also not considered. Thus, under these restricted conditions, where for a transient period of time the tissue temperature rise is linear with time of exposure, an attempt can be made to estimate what might be called a total microwave thermal dose delivered to the model (a product of exposure time and absorbed energy flux).

The use of such information to propose standards or limits for human exposure to microwaves, however, should be made carefully because of the obvious variables and assumptions involved. Specifying the maximum tolerance dose (watt-min/cm^2) for humans must incorporate biological studies to determine what tissue temperatures are allowable for any exposure time. A corresponding study must be done to find what tissue temperature elevation rates are associated with these maximum allowable tissue or body temperatures.

Several studies have been reported that deal with the effects of heat stress in humans (26, 27). These data, as applied to the case of microwave heating, have been used to illustrate the necessity of lowering exposure limits in other than ideal environmental circumstances (28). However, in light of the restrictions imposed, it is still possible to examine the thermal load placed on various tissues in the model system. These estimates provide a means of visualizing, in an approximate manner, the heating that will occur in living tissue systems of humans.

Thermal loads in various layers of the stratified model tissue system may be evaluated in terms of maximum temperature excursions during the irradiation time. In general the thermal energy imparted

to the muscle tissue is related to a corresponding temperature rise by

$$Q_M = m_M c_M \Delta T_M$$

where: Q_M = energy input to muscle during specified time

m_M = mass of muscle tissue absorbing Q_M

c_M = specific heat capacity of muscle tissue

ΔT_M = temperature excursion of muscle in degrees C during time of energy input

This relation holds for times which are short compared with the thermal diffusion time constants of the model; it assumes (1) that adiabatic conditions prevail, and (2) the energy distribution and temperature rise in the mass m_M is uniform. These conditions, of course, do not typify the situation in reality; however, for estimation purposes only the equation is reasonably accurate.

Since, generally, heat development per unit volume is the quantity computed, the above energy relation can be written for fat and muscle tissues as:[1]

$$Q_F = \rho_F V_F c_F \Delta T_F$$

$$Q_M = \rho_M V_M c_M \Delta T_M$$

Here the ρ's and V's are the densities and volumes for the two tissues. The fractional temperature rise, then, of the fat with respect to muscle is

$$\frac{\Delta T_F}{\Delta T_M} = \frac{Q_F}{\rho_F V_F c_F} \cdot \frac{\rho_M V_M c_M}{Q_M}$$

---

[1] Since, strictly, heat development per unit volume is a function of the spatial coordinates, here Q(x),

$$Q(x) = \rho \; c \; \Delta T(x)$$

where T(x) is the temperature accurately expressed as a depth or coordinate function. The total energy in the fat or muscle is then obtained by integration, not simple multiplication as implied above. Here, only a very simplified estimation process is discussed.

for the time during which the Q's are delivered. If the unit of volume is chosen the same in both cases and the Q_F delivered in a given time is related to the Q_M delivered in the same time as

$$Q_F = F\, Q_M$$

where F is the fraction of Q_M that Q_F represents, then

$$\frac{\Delta T_F}{\Delta T_M} = F\, \frac{\rho_M c_M}{\rho_F c_F}$$

Thus, if the tissues are initially at the same temperature, the maximum temperature elevation attainable in the fat medium can be expressed as some part of the maximum temperature elevation attainable in the underlying muscle tissue.

$$\Delta T_{fat}^{MAX} = F\, \frac{\rho_M c_M}{\rho_F c_F}\, \Delta T_{muscle}^{MAX}$$

If it is desired to find the same relation for a model with skin as well, then

$$\Delta T_{skin}^{MAX} = G\, \frac{\rho_M c_M}{\rho_S c_S}\, \Delta T_{muscle}^{MAX}$$

Here G is the factor relating the ratio of maximum heat development rate within skin to that in muscle. ρ_S and c_S are the density and specific heat capacity, respectively, for skin. Values given in Table 5 for ρ and c for the various tissues are taken from the literature (29).

TABLE 5. DENSITIES AND HEAT CAPACITIES OF VARIOUS TISSUES

Tissue	ρ (gm/cm^3)	c (cal/gm$^{\circ}$C)
Skin	1.20	0.81
Fat	0.92	0.55
Muscle	1.27	0.91

Computations for tissue volume heat development rates were programmed on a computer for a variety of tissue dimensions. The maximum values of the heat development rates in the fat and skin layers, normalized with respect to those in the muscle, F and G respectively, were determined, multiplied by the appropriate ratios of ρ and c, and plotted in Figures 18 and 19 as functions of fat thickness. Figure 18 refers to a two layer system and figure 19 gives the results for a three layer system in which the skin thickness is set at 0.2 cm. From these curves the relationship between the various maximum tissue temperatures can be determined in terms of the greatest temperature excursion occuring in the muscle layer. The ordinate value in these figures is simply the ratio of the maximum temperature excursion in either skin or fat to that in muscle. From Figure 18 it is determined that in a fat muscle system, the greatest temperature elevation in the fat layer will be the same as that in the underlying muscle, provided the fat is about 1.8 cm. thick and about twice as great with a fat thickness of 4.6 cm. These figures are for an idealized case which does not incorporate thermal loss or conduction within the tissue; in light of these simplications, the temperatures implied will be high. In the case of three-layer systems including skin, where the emissivity will introduce significant infrared radiation, the estimate may be very high compared to reality. This approximate estimation technique agrees reasonably well with the experimental maximum fat and muscle temperatures attained in work reported by Guy (30). His investigation involved the recording of thermographic images, indicating maximum tissue temperature, for various combinations of fat-muscle models exposed to several frequencies of microwave energy. Surface heating effects are very obvious in these graphs where Figure 19 c shows the impractical task of deep muscular heating with very short wavelength microwaves. Heating here is almost solely on the surface. These computations imply a rather difficult, and sometimes impractical measurement of the maximum base layer temperature in humans or laboratory animals. However, the results for the model systems should prove useful for qualitatively evaluating certain exposure situations.

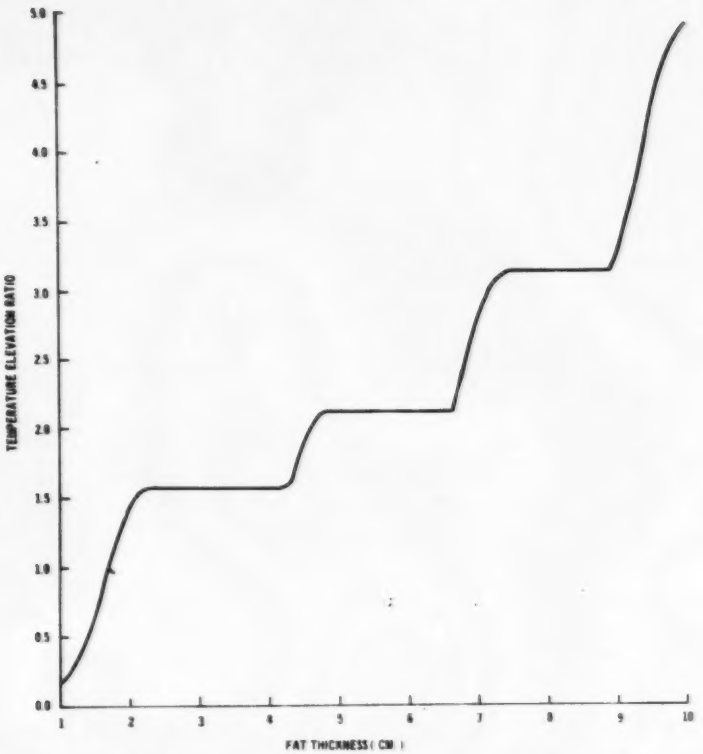

Figure 18. Maximum Tissue Temperature Elevation in Two-Component System at 2450 MHz; No Skin.

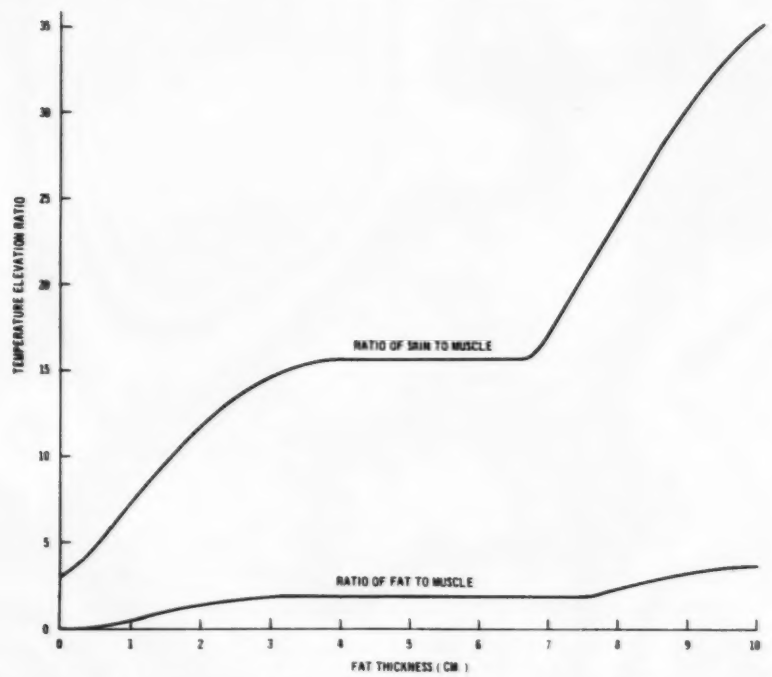

Figure 19A. Maximum Tissue Temperature Elevation in Three-Component System at 915 MHz; 0.2 cm Skin.

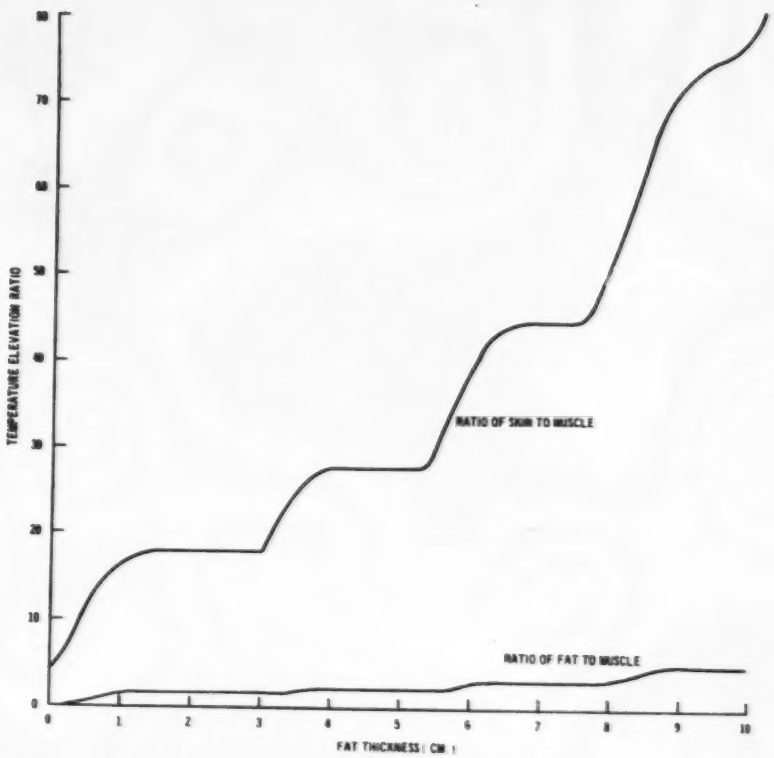

Figure 19B. Maximum Tissue Temperature Elevation in Three-Component System at 2450 MHz; 0.2 cm Skin.

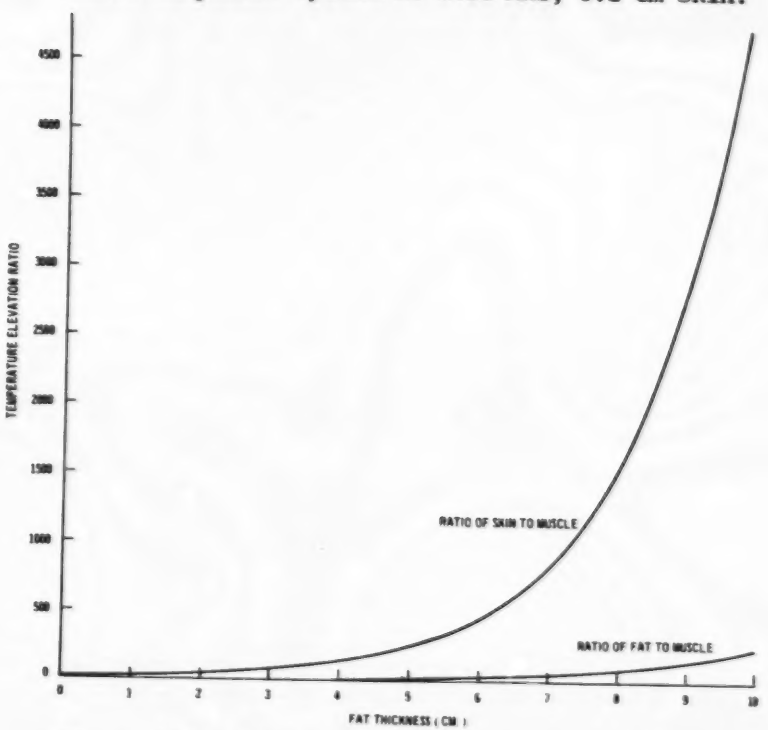

Figure 19C. Maximum Tissue Temperature Elevation in Three-Component System at 8500 MHz; 0.2 cm Skin.

SUMMARY AND CONCLUSIONS

The planar slab model for tissues is a very simplified model that is subject to a large number of constraints. The application of this model to actual human and laboratory animal dosimetric studies involves, consequently, an element of approximation when precise dose estimates are desired. Generally, actual temperature excursions experienced by the various tissues which comprise the exterior part of the anatomy will be typically lower than predicted here due to thermal exchange with blood and environment. Also, the semi-infinite slab model should not be used when dealing with structures of the anatomy characterized by significant curvatures, e.g., the head. In these cases, the curvature plays an important role in refracting the incident microwave beam with the possible development of local relative hot spots which would not have been predicted with the semi-infinite assumption.

A spherical model approximating a monkey head has recently been used to predict heating distributions within the cranial cavity (31). The approach used consisted of calculating both the scattered and interior fields for a series of concentric spherical shells. Analytical details of scattering from dielectric spheres and spherical shells are available in the literature (32 - 34). Similar investigations have also been carried out to determine effective cross sections for a range of tissue equivalent sphere sizes (33). The primary observation indicated that the cross section was critically dependent on sphere radius, again suggesting the refractive role of curved surfaces in microwave interactions. Thus, the total power extracted from a plane wave by a dielectric sphere cannot, in general, be computed simply by finding the product of incident power density in the field and shadow cross section of the sphere. These special considerations are given to reveal the complicated nature of microwave dosimetry in irregularly shaped objects. Conservative dosimetric estimates based on the semi-infinite slab model results should, therefore, take into account the greatest possible degree of power absorption.

In this report we have mathematically described a planar slab tissue model in terms of its microwave absorption characteristics. Both the total power absorption and the development of heat spatially have been examined for a wide range of tissue dimensions. The partition of this heat, fractionally, in the various tissues has been obtained, and finally the relation between maximum tissue temperature elevations in the various tissues has been determined. The following conclusions can be drawn:

1. Beam power extraction, or coupling, may vary as much as a factor of 5 over the frequency range of 915 to 8500 MHz and the possible range of tissue dimensions considered.

2. Peak heating within the base layer is at the interface between that layer and the next outermost layer. Peak heating within other overlying tissues may occur at various positions throughout the tissue, depending upon the particular combination of tissue dimensions.

3. The fractional integrated heat development within skin tissue increases with increase in frequency and increase in skin thickness.

4. Maximum temperature rise in skin and fat tissues are generally always higher than the greatest temperature excursion in the deepest lying tissue. This is due to the enhanced surface heating of a relatively lossy tissue and the ratios of the tissue specific heats.

5. Biological tissues may be broadly classified, dielectrically, either as high or low loss. Skin, muscle, blood, and similar non-fatty tissues are high loss; fat and bone are low loss. Thus, for practical purposes most biological systems may be modeled on the basis of two types of material for microwave absorption analysis.

6. The semi-infinite model is not satisfactory for objects with radii of curvature on the order of the wavelength or smaller than that of the incident energy.

References

1. Baldwin, B. R., P. C. Constant, Jr., R. W. Fetter, B. L. Jones, V. W. Klein, E. J. Martin, Jr., L. Runge, D. L. Waidelich. 14 June 1960. Survey of radiofrequency radiation hazards, Summary Report #2 (20 May 1960-19 May 1961). Midwest Research Institute, Kansas City, Missouri. Contract No. Nobs-77142, Navy, Bureau of Ships.

2. Saito, M., and H. P. Schwan. 1961. Biological effects of microwave radiation, Vol. 1, pp. 85-97, Plenum Press, New York.

3. Schwarz, G., M. Saito, and H. P. Schwan. 1965. On the orientation of non-spherical particles in an alternating electrical field. J. Chem. Phys. 43:3562-3569.

4. Saito, M., L. D. Sher, and H. P. Schwan. July 1961. RF field-induced forces on microscopic particles. Digest 4th International Conference on Medical Electronics.

5. Frey, A. 1962. Human auditory system response to modulated electromagnetic energy. J. Appl. Physiol. 17:689.

6. Marha, K., J. Musil, and H. Tuha. 1968. Electromagnetic fields and the living environment. State Health Publishing House, Prague, Czechoslovakia.

7. Letanet, A. A., and Z. V. Gordon (ed.). 1960. The biological action of ultrahigh frequencies, Moscow. Translated by U.S. Joint Publications Research Service, JRPS:12471, February 1962, Washington, D.C.

8. Presman, A. S. 1970. Electromagnetic fields and life, Plenum Press, N.Y. - London.

9. Schwan, H. P., E. L. Carstensen, and K. Li. September 1953. Heating of fat-muscle layers by electromagnetic and ultrasonic diathermy. Transactions of the AIEE, p. 483.

10. Livenson, A. R. 1966. Determination of the coefficient of reflection for multilayered systems of biological tissues in the microwave range. Translated from Russian in 1968, Translation Division, Foreign Technology Division, Wright Patterson AFB, Ohio. AD681254.

11. Schwan, H. P., and K. Li. November 1956. Hazards due to total body irradiation by radar. Proc. I.R.E. 44:1572-1581.

12. Schwan, H. P., and G. M. Piersol. 1954. The absorption of electromagnetic energy in body tissues, Part I. Am. J. Phys. Med. 33:371-404.

13. von Hippel, A. R. 1954. Dielectrics and waves. The M.I.T. Press, Cambridge, Massachusetts.

14. Frohlich, H. 1949. Theory of dielectrics. Clarendon Press, Oxford.

15. Schwan, H. P. 1957. Electrical properties of tissue and cell suspensions, p. 147-209. In Advances in biological and medical physics, Tobias and Lawrance (eds.), Vol. 5, Academic Press, New York.

16. Schwan, H. P. 1958. Biophysics of diathermy, p. 55-115. In Therapeutic heat, S. Licht (ed.). Elizabeth Licht, Publisher, New Haven, Connecticutt.

17. Cook, H. F. October 1951. The dielectric behaviour of some types of human tissues at microwave frequencies. Brit. J. Appl. Phys. 2:295.

18. England, T. S., and N. A. Sharples. 1949. Dielectric properties of the human body in the microwave region of the spectrum. Nature 163:487-488.

19. Schwan, H. P., and K. Li. 1953. Capacity and conductivity of body tissues at ultrahigh frequencies. Proc. I.R.E. 41:1735-1740.

20. Sharpe, C. B. 1960. A graphical method for measuring dielectric constants at microwave frequencies. Trans. I.R.E., MTT-8, p. 155.

21. Roberts, S., and A. von Hippel. 1946. A new method of measuring dielectric constant and loss in the range of centimetre waves. J. Appl. Phys. 17:610.

22. Harvey, A. F. 1963. Microwave engineering. Academic Press, London-New York, p. 233-270.

23. Gilmore, J. F. May 1966. Measurements of dielectric materials with the precision slotted line. General Radio Experimenter, published by General Radio Company, West Concord, Massachusetts.

24. Livenson, A. R. 1964. Electrical parameters of biological tissue in the microwave range, Report II. Methods of gauging electrical parameters of biological tissue. Translated from Russian by Joint Publications Research Service, JPRS:26424, 16 September 1964, Washington, D. C.

25. Stratton, J. A. 1941. Electromagnetic theory. McGraw-Hill Book Company, New York.

26. Belding, H. A., and T. R. Hatch. August 1955. Index for evaluating heat stress in terms of resulting physiological strains. Heating, Piping, Air Conditioning 26:129-136.

27. Haines, G. F., and T. R. Hatch. November 1952. Industrial heat exposures - Evaluation and control. Heating and Ventilating, p. 94-104.

28. Mumford, W. W. 1969. Heat stress due to RF radiation. Proc. I.E.E.E. 57:172-177.

29. Lipkin, M., and J. D. Hardy. 1954. Measurement of some thermal properties of human tissues. J. Appl. Physiol. 7:212-217.

30. Guy, A. W., J. F. Lehmann, J. A. McDougall, and Carrol C. Sorenson. 1968. Studies on therapeutic heating by electromagnetic energy, p. 26-45. In Thermal problems in biotechnology, American Society of Mechanical Engineers, Heat Transfer Division, New York.

31. Shapiro, A. R., R. F. Lutomirski, and H. T. Yura. September 1970. Induced fields and heating within a cranial structure irradiated by an electromagnetic plane wave, Technical Report P-4458-1. The Rand Corporation, 1700 Main Street, Santa Monica, California.

32. Anne, A., M. Saito, O. M. Salati, and H. P. Schwan. 1961. Relative microwave absorption cross sections of biological interest. In Proceedings of the fourth annual tri-service conference on the biological effects of microwave radiation, Vol. 1, Plenum Press, New York, p. 153-176.

33. Aden, A. L., and M. Kerker. 1951. Scattering of electromagnetic waves from two concentric spheres. J. Appl. Phys. 22:601-605.

34. Chu, G., D. G. Dudley, and T. W. Bristol. 1969. Interaction between an electromagnetic plane wave and a spherical shell. J. Appl. Phys. 40:3904-3914.

35. von Hippel, A. 1954. Dielectric materials and applications, John Wiley and Sons, New York.

APPENDIX A

Verification that $\tan \delta = \frac{60\lambda_o}{K'\rho}$

Given:

ρ = resistivity

λ_o = free space wavelength

ω = angular frequency

f = frequency

ε_o = permittivity of free space

μ_o = permeability of free space

c = speed of light

$Z_o = \sqrt{\frac{\mu_o}{\varepsilon_o}} = 120\pi$ ohms = 377 ohms

K' = relative permittivity of medium

K'' = relative loss factor of medium

$C^2\mu_o\varepsilon_o = 1$

From:

$$K'' = \frac{1}{\rho\omega\varepsilon_o} \qquad \rho = \frac{1}{K''\omega\varepsilon_o}$$

Thus:

$$\frac{60\lambda}{K'\rho} = \frac{60\lambda}{K'\frac{1}{K''\omega\varepsilon_o}} = \frac{K''}{K'} 60\lambda\varepsilon_o = \frac{K''}{K'} 60\lambda_o 2\pi f\varepsilon_o = \frac{K''}{K'} 120\pi\lambda_o f\varepsilon_o$$

$$= \frac{K''}{K'} Z_o\lambda_o \frac{c}{\lambda_o} = \frac{K''}{K'} Z_o c\varepsilon_o = \frac{K''}{K'} Z_o \frac{\varepsilon_o}{\sqrt{\mu_o\varepsilon_o}}$$

$$= \frac{K''}{K'} Z_o \sqrt{\frac{\varepsilon_o}{\mu_o}} = \frac{K''}{K'} Z_o \frac{1}{Z_o} = \frac{K''}{K'}$$

Thus:

$$\tan \delta = \frac{60\lambda_o}{K'\rho} = \frac{K''}{K'}$$

APPENDIX B

Wavelength Reduction in a Dielectric Material

The index of refraction, n, is related to the velocity of electromagnetic waves in vacuum and a dielectric material by

$$n = \frac{c}{v}$$

where:

c = velocity of light

v = phase velocity of the wave in a dielectric medium.

Now:

$$n = \frac{c}{v} = \frac{\frac{1}{\sqrt{\mu_o \varepsilon_o}}}{\frac{1}{\sqrt{\mu_m \varepsilon_m}}} = \sqrt{\frac{\mu_m \varepsilon_m}{\mu_o \varepsilon_o}}$$

If μ_m/μ_o is 1 as in the case of biological materials, then

$$\frac{c}{v} = \sqrt{K^*_m} \qquad \text{or, } v = \frac{c}{\sqrt{K^*_m}}$$

Since $v = f\lambda_m$,

$$\lambda_m = \frac{c}{f\sqrt{K^*_m}}$$

If f is in units of MHz, then

$$\lambda_m \text{ (cm)} = \frac{30{,}000}{\sqrt{K^*_m}\,[\,f \text{ (MHz)}\,]}$$

The magnitude of K^*_m is used under the radical sign. For materials with low loss, such as fat, direct use of K' rather than the magnitude of K^*_m will yield fairly accurate results.

APPENDIX C

Verification that $\alpha\beta = \frac{\mu\sigma\omega}{2}$

Given:

$$\gamma = j\omega\sqrt{\epsilon^*\mu^*} \qquad (1)$$

$$\gamma = \alpha + j\beta \qquad (2)$$

for biological tissues $\mu^* = \mu_o = \mu_o' - j0 = \mu_o'$

thus

$$\gamma = j\omega\sqrt{(\epsilon' - j\epsilon'')(\mu_o')} \qquad (3)$$

Square (2) and (3) and set equal. Equate imaginary and real parts to get:

$$2\alpha\beta = \omega\mu_o'\sigma \qquad \text{(Imaginary part)} \quad (4)$$

$$\beta^2 - \alpha^2 = \omega^2\mu_o'\epsilon' \qquad \text{(Real part)}$$

From (4)

$$\alpha\beta = \frac{\mu\sigma\omega}{2}$$

• U. S. GOVERNMENT PRINTING OFFICE : 1972—484-484/163